



Forschungszentrum Karlsruhe
in der Helmholtz-Gemeinschaft

Wissenschaftliche Berichte
FZKA 7382

Behavior of the Melt Pool in the Lower Plenum of the Reactor Pressure Vessel - Review of Experimental Programs and Background of the LIVE Program

F. Kretzschmar, B. Fluhrer

**Institut für Kern- und Energietechnik
Programm Nukleare Sicherheitsforschung**

April 2008

Forschungszentrum Karlsruhe

in der Helmholtz-Gemeinschaft

Wissenschaftliche Berichte

FZKA 7382

**Behavior of the Melt Pool in the Lower Plenum of
the Reactor Pressure Vessel -
Review of Experimental Programs and Background
of the LIVE Program**

F. Kretzschmar, B. Fluhrer

Institut für Kern- und Energietechnik

Programm Nukleare Sicherheitsforschung

Forschungszentrum Karlsruhe GmbH, Karlsruhe

2008

Für diesen Bericht behalten wir uns alle Rechte vor

Forschungszentrum Karlsruhe GmbH
Postfach 3640, 76021 Karlsruhe

Mitglied der Hermann von Helmholtz-Gemeinschaft
Deutscher Forschungszentren (HGF)

ISSN 0947-8620

urn:nbn:de:0005-073824

ZUSAMMENFASSUNG

Das Verhalten eines Schmelze-Pools im unteren Plenum eines Reaktordruckbehälters – Überblick über experimentelle Programme und Grundlagen für das LIVE-Versuchsprogramm

Die Rückhaltung der Kernschmelze im unteren Plenum des Reaktordruckbehälters (RDB) ist eine der in den letzten Jahren intensiv untersuchten Strategien, um einen hypothetischen Kernschmelzunfall zu beherrschen. In verschiedenen Institutionen weltweit wurden deshalb Experimente durchgeführt, um diese Strategie, welche bereits für das KKW Loviisa (Finnland) und den AP 600 (USA) genehmigt wurde, weiterzuentwickeln. Die wichtigsten Experimente waren dabei:

- COPO-Experimente in Fortum Nuclear Services und CEA (Frankreich)
- BALI-Experimente bei CEA (Frankreich)
- SIMECO-Experimente im KTH (Schweden)
- ACOPO-Experimente an der Universität von Kalifornien, Santa Barbara (USA)
- RASPLAV-Experimente am Kurchatow-Institut (Russland)

Diese Untersuchungen wurden nicht nur durchgeführt, um die Möglichkeit der Schmelze-Rückhaltung im RDB zu untersuchen, sondern auch, um das Verhalten eines Schmelzepools im unteren Plenum des RDB grundlegend zu verstehen. Die Ergebnisse dieser Untersuchungen wurden dazu verwendet, Modelle bzw. Korrelationen zu ermitteln, die in Rechencodes zur Untersuchung schwerer Unfälle verwendet werden können.

Das Forschungszentrum Karlsruhe beteiligt sich mit der Versuchsanlage LIVE (Late In-Vessel Phase Experiments) an diesen Untersuchungen.

Das Hauptziel dieses Berichtes ist es, die Ergebnisse anderer experimenteller Programme zum Schmelzeverhalten im unteren Plenum des RDB's zusammenzufassen und damit ein Bild des derzeitigen Kenntnisstandes zu geben. Weiterhin soll gezeigt werden, wie die noch offenen Fragen im LIVE-Programm untersucht werden können.

ABSTRACT

Retention of core melt in the lower plenum of the reactor pressure vessel (RPV) is one of the severe accident management strategies, which were investigated quite intensely in the last years. In several organizations over the world experiments were conducted to enhance this strategy which has already been approved to be a part of the severe accident management strategy for the Loviisa plant (Finland) and for the Westinghouse AP-600 design. The most important experiments to reach this goal were:

- COPO experiments at Fortum Nuclear Services and CEA (France)
- BALI experiments at CEA (France)
- SIMECO experiments at KTH (Sweden)
- ACOPO experiments at the University of California, Santa Barbara (USA)
- RASPLAV experiments at the Kurchatov Institute (Russia)

These investigations were performed not only to study the possibility of retaining the core melt inside the reactor pressure vessel (as an accident management measure) but also to understand the fundamental behavior of the molten pool inside the RPV (for homogeneous and stratified configuration of the molten pool). With the help of the results of these experiments we want to identify models and correlations, which can be used in severe accident computer codes.

Forschungszentrum Karlsruhe is involved in this research with the experimental LIVE (Late In-Vessel Phase Experiments) program.

The major objective of the current report is to summarize the findings obtained in earlier experimental programs on melt behavior in the RPV in order to provide a coherent picture of the state of knowledge and to identify the remaining uncertainties. Further on the report will show how these uncertainties shall be investigated in the LIVE experimental program.

CONTENTS

1	INTRODUCTION AND BACKGROUND	1
2	KEY FEATURES OF THE MELTDOWN / RELOCATION BEHAVIOR	3
3	SURVEY OF TEST FACILITIES AND EXPERIMENTAL PROGRAMS	5
3.1	<i>COPO experiments.....</i>	5
3.1.1	The COPO I facility	5
3.1.2	The COPO II facility	7
3.2	<i>BALI experiments</i>	10
3.3	<i>SIMECO experiments</i>	13
3.4	<i>ACOPO experiments</i>	17
3.5	<i>RASPLAV experiments</i>	20
4	SURVEY OF KEY PROBLEMS CONCERNING THE CORE MELT IN THE LOWER PLENUM.....	24
5	The LIVE TEST FACILITY TO INVESTIGATE MELT BEAVIOR IN THE RPV LOWER HEAD	28
5.1	<i>Description of the LIVE test facility.....</i>	28
5.2	<i>Simulant materials for LIVE experiments</i>	33
5.3	<i>Phenomena to be investigated in the LIVE test facility.....</i>	36
5.4	<i>Planned experiments in the LIVE test facility</i>	38
5.4.1	Experiments with water at different pool heights and power densities	38
5.4.2	Experiments with water in the LIVE vessel and in a slice with the same radius	39
5.4.3	Cooling down hot water in the LIVE vessel like in ACOPO experiments	39
5.4.4	Experiments with NaNO ₃ -KNO ₃ to confirm the results in the SIMECO facility	39
5.4.5	Experiments with NaNO ₃ -KNO ₃ at different power densities	42
5.4.6	Experiments with NaNO ₃ -KNO ₃ at different heights of the melt	42
5.4.7	Experiments with NaNO ₃ -KNO ₃ at different cooling conditions.....	42
5.4.8	Experiments with NaNO ₃ -KNO ₃ at different compositions of the melt.....	42
5.4.9	Experiments with NaNO ₃ -KNO ₃ in the LIVE vessel and in a slice with the same radius	43
5.4.10	Experiments with NaNO ₃ -KNO ₃ with different time histories	43
5.4.11	Experiments with NaNO ₃ -KNO ₃ with different initial pouring temperatures of the melt.....	43
5.4.12	Experiments with NaNO ₃ -KNO ₃ with different pouring masses	43
5.4.13	Experiments with NaNO ₃ -KNO ₃ with different melt pouring positions	44
5.4.14	Experiments with NaNO ₃ -KNO ₃ with a gradual pouring of melt	44

6	REFERENCES	45
Appendix A	Experimental facilities.....	49
Appendix B	EURSAFE Research Issue and Rationale for Selection (from [Sar07])	53

LIST OF FIGURES

Fig. 3-1: Schematic of the COPO facility (from [Kym03])	5
Fig. 3-2: The cooling units of the COPO facility (from [Kym03])	6
Fig. 3-3: Upward, downward and sideward heat flow from a fluid with internal heat sources in a rectangular cavity (from [May75])	7
Fig. 3-4: Schematic of the COPO II-Lo facility (from [Hel99])	9
Fig. 3-5: Schematic of the COPO II-AP facility (from [Hel99]).....	9
Fig. 3-6: The BALI test section (from [Ber98]).....	10
Fig. 3-7: Upward heat transfer ACOPO – BALI - COPO I – COPO II comparison (from [Ber98])	11
Fig. 3-8: Average lateral heat flux in metal layer experiments of BALI (from [Ber98]).....	12
Fig. 3-9: Schematic of the SIMECO facility (from [Ste05]).....	13
Fig. 3-10: Location of the thermocouples in the SIMECO facility (from [Ste05]).....	14
Fig. 3-11: Main dimensions of the SIMECO vessel (from [Ste05])	14
Fig. 3-12: Miscibility gap for the mixture of Benzyl benzoate and Parafin oil (from [The00]).....	15
Fig. 3-13: Transient during the mixing process (thermocouple near the top of the pool), (from [The00]).....	16
Fig. 3-14: Schematic of the ACOPO test vessel with individual cooling unit (from [The97]).....	17
Fig. 3-15: Key construction details and instrumentation (from [The01])	18
Fig. 3-16: Schematic of the ACOPO experiment (from [The01]).....	18
Fig. 3-17: Upward heat transfer from ACOPO compared to the Steinberner-Reineke correlation (from [The01]).....	19
Fig. 3-18: System of coordinates adapted in RASPLAV-A-salt experiments (from [Asm98b]).....	20
Fig. 3-19: Layout of the thermocouples in the melt pool (from [Asm98b])	21
Fig. 3-20: Ratio of Nusselt number at angle θ to the average Nusselt number	23
Fig. 5-1: Melt retention in the lower head (LIVE1)	28
Fig. 5-2: Melt relocation to the lower head (LIVE2)	29
Fig. 5-3: LIVE test vessel (from [Fzk08]).....	29
Fig. 5-4: Scheme of the LIVE test facility (from [Fzk08])	30
Fig. 5-5: LIVE instrumentation plug (from [Mia07])	30
Fig. 5-6: LIVE volumetric heating system (from [Mia07]).....	31
Fig. 5-7: LIVE heating furnace	32
Fig. 5-8: Phase diagram of the $\text{KNO}_3\text{-NaNO}_3$ melt.....	33
Fig. 5-9: Phase diagram of the $\text{V}_2\text{O}_5\text{-ZnO}$ melt.....	34
Fig. 1-1: Ratio of the area at the top of the pool to the area at the interface with the wall vs. the normalized height of the pool	38
Fig. 1-2: Experimental results in SIMECO tests with $\text{NaNO}_3\text{-KNO}_3$ salts	40
Fig. 1-3: Rayleigh numbers vs. Temperature for the non-eutectic (20%-80%) $\text{NaNO}_3\text{-KNO}_3$ mixture	41
Fig. 1-4: Rayleigh numbers vs. Temperature for the eutectic (50%-50%) $\text{NaNO}_3\text{-KNO}_3$ mixture .	41

LIST OF TABLES

Table 4-1: Phenomena associated with In-Vessel Retention issue (from [Asm01])	24
Table 5-1: Material properties of NaNO ₃ -KNO ₃ mixtures.....	35
Table 1-1: Experimental results in SIMECO tests with NaNO ₃ -KNO ₃ salts	39

1 INTRODUCTION AND BACKGROUND

In case of a severe accidental situation that may occur in a nuclear reactor, accident management measures have been developed to bring the situation under control, which means, to prevent a damage of the reactor core. Nevertheless, a very low remaining risk exists that the reactor core can not be cooled successfully due to cumulative safeguard failures. This would then lead to a heat up and melting of core elements and structural materials. In this situation the RPV can fail and the core melt is discharged onto the basement of the containment. But even in such a case, a significant release of radioactive material to the environment due to the meltthrough of the basement should be excluded. Therefore several strategies were developed to avoid the release of the radioactive material to the environment.

In the first group of strategies the core melt is cooled and stabilized in the containment, after the Reactor Pressure Vessel (RPV) has failed. This strategy is realized e.g. in the EPR concept of AREVA and in the Russian VVER-1200 design. However, this strategy can not be applied to existing reactors, because the retrofitting of a spreading area for the core melt or of a core catcher construction requires substantial structural changes in the reactor buildings, or is even impossible.

Another strategy is to retain the core melt in the lower head of the RPV. This requires an outside cooling of the RPV by water in the reactor cavity. Such an in-vessel retention concept has been approved to be part of the accident management strategy for IVO's Loviisa plant [Kym97]. It is also foreseen in the design of the AP-600, the AP-1000 and BWR-1000. Flooding of the reactor cavity is also an accident management measure in some of the existing boiling water reactors.

This strategy can also be an option for the core melt retention in existing NPP's.

To investigate the thermal and mechanical loadings on the RPV after the core melt has relocated into the lower plenum and to define initial conditions for the event when the lower head of the RPV fails in case of inadequate cooling, several research programs were started.

In these programs several aspects of the core melt behavior in the lower plenum have been investigated.

The goals of all these programs were:

- To improve the understanding of different phenomena influencing the melt behavior in the lower plenum (e.g. crust formation, gap cooling at the vessel wall, phase separation etc.).
- To develop models, which can be implemented into severe accident codes (e.g. MELCOR, MAAP, SCDAP/RELAP, ICARE/CATHARE, ASTEC).
- To define accident management procedures which can mitigate the consequences of the core melt accident in existing reactors.

FZK participates in this research with the experimental LIVE (Late- In-Vessel -Phase- Experiments)- program. In the frame of LIVE it is foreseen to improve the understanding of the transient processes in the lower plenum during and after the core melt relocation into the lower plenum.

The following objectives are part of the LIVE program:

- Investigation of the influence of the melt relocation mode on heat flux distribution through the vessel wall.
- Study of temperature distribution in the bulk of the melt undergoing natural convection.
- Investigation of crust formation and growth at the pool/vessel wall boundary and its influence on the heat flux distribution.
- Comparison of the 3D results with earlier experiments performed in 2D slice geometry (BALI, SIMECO, COPO, RASPLAV).
- Confirmation of the ACOPO philosophy.

The first three points are certainly the focus of the experimental program, because in this field uncertainties still exist.

The intention of this report is to describe the main experimental facilities in the research field of core melt behavior in the lower plenum and to summarize the results obtained in earlier experimental programs. Furthermore the report defines boundary conditions and objectives for future experiments in the LIVE test facility.

2 KEY FEATURES OF THE MELTDOWN / RELOCATION BEHAVIOR

In the very unlikely case of a severe accident with core meltdown there is a potential for material relocation into the lower plenum of the reactor pressure vessel. Depending on the reactor design and the accident scenario one can consider two different relocation mechanisms:

- Coherent relocation:
Under certain conditions, melt relocation from the core into the lower plenum could occur relatively coherently. But this requires the formation of a large melt pool in the core and an uninterrupted release of most of the molten material during a short period.
The duration of the relocation process depends on several factors, such as:
 - the relocated mass
 - the location of the molten pool crust breach
 - the melt flow area and the hole ablation rate
 - the presence of several structures in the core
- Gradual relocation:
If there are no thermal or mechanical factors causing melt retention and melt pool formation in the lower parts of the core, the melt relocation from the core into the lower plenum can proceed gradually according to the melt down of the core material within the core.

There is a large consensus in the international community that gradual relocation is unlikely to occur. The coherent melt relocation scenario seems to be much more likely for light water reactors. One reason is that the large mass of the structures at the bottom of the core withstand the thermal attack of the core melt for a relatively long time. They also form a heat sink, where the core material can refreeze. This crust stabilizes the melt pool within the core for a certain time. Another reason is that there are “wet-core”-conditions (presence of water in the bottom of the core at the time of core degradation) in most scenarios. On the one hand that leads to a refreezing of molten material at the bottom of the core, on the other hand the produced steam oxidizes molten core material in the upper part of the core. This oxidized material has a higher melting point, which also stabilizes the melt pool.

The TMI-2 accident also proceeded along this melt relocation scenario. A large melt pool has been formed in the core region and after a breach in the side wall of the pool crust the melt has been released into the lower plenum [And89].

The gradual relocation may be potentially relevant for VVER-440 designs with its large steel-made control assemblies in the core, which can be molten already at the time of fuel assembly degradation, providing a preferential way for downward material relocation into the lower plenum [Band98], [Band01].

The main initial parameters at the instant of melt release from the core to the lower plenum are:

- Time of crust failure and first relocation of core melt into the lower plenum
- Mass of relocated core melt
- Composition of the core melt at the moment of the relocation
- Ablation rate after crust breach
- Temperature of the relocated core melt

Bandini wrote in [Band01]: “From the point of view of timing, pouring rate and amount of involved materials the melt relocation process is an almost completely unresolved issue. Further investigation should be addressed to evaluate molten pool crust behavior, and melt interactions with core surrounding and support structures, which may influence the pouring rate and transfer mode of molten material to the lower head of the vessel.” This situation has not changed so far.

3 SURVEY OF TEST FACILITIES AND EXPERIMENTAL PROGRAMS

Several experimental programs were conducted to investigate the behavior of the core melt in the lower plenum. This chapter provides information on experimental setup and main results obtained in these programs.

3.1 COPO experiments

The COPO experiments were performed by Fortum Nuclear Services, Finland and CEA/DRN (Grenoble), France.

The experiments were conducted in two facilities, the COPO I - and the COPO II - facility.

3.1.1 The COPO I facility

The COPO I facility is a two-dimensional “slice” of the Loviisa lower head (VVER-440 type), including a portion of the cylindrical vessel wall. This allows a well-controlled, uniform heating by volumetric Joule heating (the electrical resistance of the fluid causes its heat up when a current flows through it) and is convenient for achieving large characteristic length scales and thus large Rayleigh numbers (10^{15} - 10^{16}). The test section is illustrated in Fig. 3-1 and the shape is shown in more detail in Fig. 3-2. It is geometrically similar to Loviisa lower head, it measures a span of 1.77 m and allows a maximum pool depth of 0.8 m (1:2 scale). The thickness of the slice is 0.1 m.

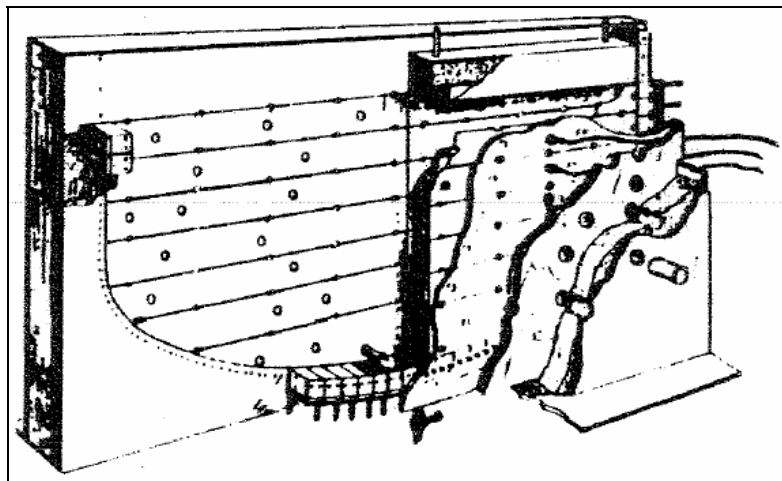


Fig. 3-1: Schematic of the COPO facility (from [Kym03])

The flats of the test section are built from poly-carbon plates and are heavily insulated.

On the inside the plates are lined by seven pairs of electrode strips. At selected locations both electrodes and insulation have 20 mm holes to gain visual access to the fluid. The current through each electrode can be individually adjusted, if necessary, in order to produce uniform volumetric heating.

The side and bottom walls consist of a 57 separate cooling units, as illustrated in Fig. 3-2.

Each cooling unit consists of 50-mm-thick brass wall electrically insulated from the pool by a 0.1-mm-thick teflon tape. Coolant water circulates on the back side of the brass walls. The units are divided into three groups and the flow is adjusted evenly among the units of each group to obtain a nearly isothermal boundary. The top surface cooling is provided by two units (58 and 59). They are constructed out of aluminum sheet and are electrically insulated from the pool by a thin aluminum-oxide coating. The cooling water passes through heat exchangers and its flow rate is measured by an electromagnetic flow meter. The oxidic pool is simulated by a $\text{ZnSO}_4\text{-H}_2\text{O}$ solution [Kym03]. The material properties for this fluid are not given by the authors.

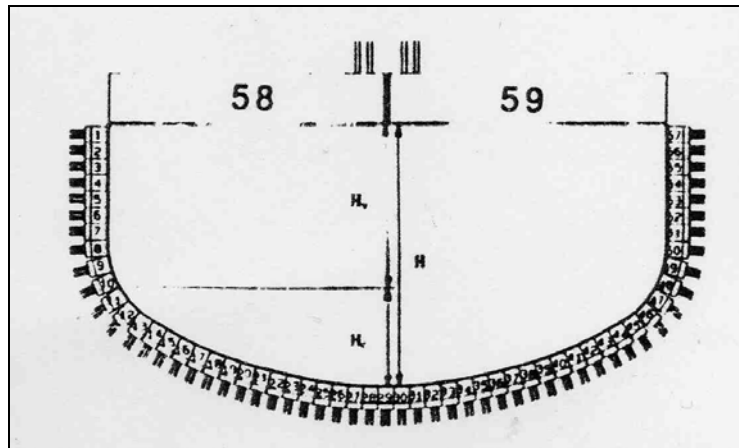


Fig. 3-2: The cooling units of the COPO facility (from [Kym03])

In the experiments heat flux distributions at isothermal boundaries were measured. This was done for two different pool heights. The conclusions were:

1. The heat flux at the vertical portion of the side wall is essentially uniform and predicted well by
2. The downward heat flux strongly depends on the position along the curved wall, and for the shape considered it seems to be independent of the presence and extent of the liquid pool (contained by the vertical sidewall) portion above it.
3. The heat flux to the top boundary is somewhat underestimated by the correlation of Steinberner and Reineke

$$Nu_{hr} = 0.85 \cdot Ra^{0.19} \quad \bar{\tau}$$

$$Nu_{up} = 0.345 \cdot Ra^{0.233} \quad \bar{\tau}$$

In [Kym03], it is referred to [Ste78] for these two correlations. But the correlation for Nu_{up} is not given there. Therefore we refer to [May75] (an english reference could not be found) for this correlation. We also point out that the scope of application of the Steinberner-Reineke correlation was originally limited to $Ra=10^7$ (see Fig. 3-3).

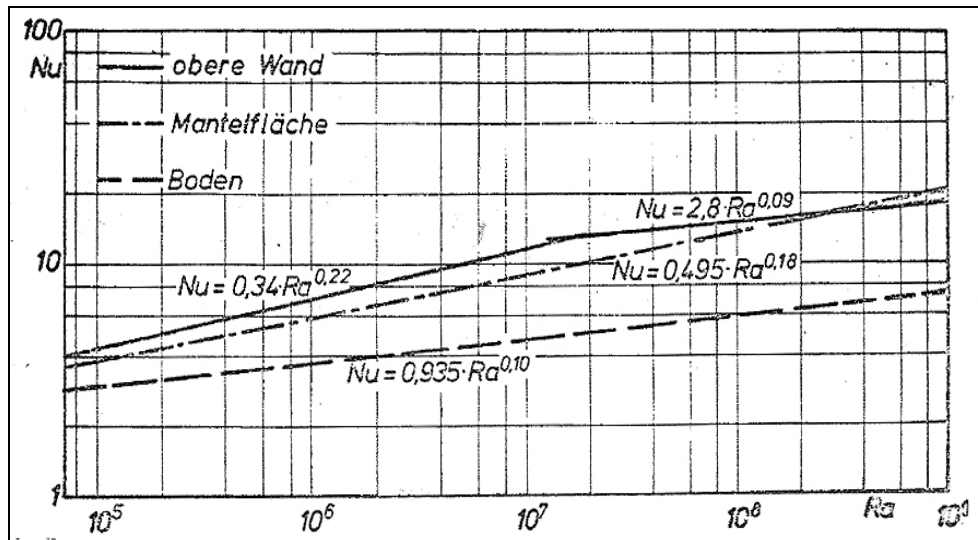


Fig. 3-3: Upward, downward and sideward heat flow from a fluid with internal heat sources in a rectangular cavity (from [May75])

3.1.2 The COPO II facility

Two geometrically different versions of the COPO II facility have been constructed: one version called COPO II-Lo, which follows the shape of the lower head of the RPV of a VVER-440 reactor (torispherical bottom) similar to COPO I and a version called COPO II-AP having a semicircular shape and thus modeling the RPV bottom of a western PWR. In both facilities, the molten corium pool in the lower head of the RPV is simulated by a two-dimensional slice of it in linear scale 1:2. The width of the slice is 94 mm. The simulant fluid for corium is a $\text{ZnSO}_4\text{-H}_2\text{O}$ solution (as in COPO I). The volumetric heat generation is produced by Joule heating (as in COPO I). Maximum continuous heating power is 25 kW.

Heat fluxes are obtained by measuring the temperature gradients in the cooling units. The upper cooler is divided into 25 cooling units in COPO II-Lo and into 26 cooling units in COPO II-AP. The spatial resolution is thus 50 – 75 mm.

A distinctive feature in the COPO II facilities is the cooling arrangement in which liquid nitrogen is circulated on the backside of the aluminum walls of the pool. The use of liquid nitrogen leads to formation of ice on the inside of the boundaries. Because of the ice, the boundary conditions of the pool are ideally isothermal and, also, the temperature difference in the pool can be made sufficiently large to allow possible effects of temperature dependent fluid properties to become observable.

COPO II features an option for stratified pool tests. Two layers to be used are $\text{ZnSO}_4\text{-H}_2\text{O}$ solution at the bottom as a heat generating layer and distilled water on top of it as non heat generating layer. The layers are separated by a 2-mm-thick aluminum sheet, which is insulated electrically by an aluminum oxide coating [Hel99]. This sheet models a crust, which also would be formed between an oxidic and a metallic layer in the core melt.

Fig. 3-4 and Fig. 3-5 show the schematics of COPO II-Lo and COPO II-AP.

The COPO II results for the upward heat transfer coefficients were consistent with the BALI results (see next section). However, they showed higher values as expected from the Steinberner-Reineke correlation and also higher values than the ACOPO experiments.

It was shown that in experiments with a crust at the top of the pool the Nusselt number was remarkably higher (20-30%) than in experiments with an ice-free upper boundary. An ultimate explanation for this effect is still outstanding, but possible explanations are given in [Hel99]:

1. The density gradient inversion of water near the crust boundary could influence the heat transfer from the fluid to the ice. But in one experiment with no ice boundary, the temperature of the upper surface was at the freezing point of water or possibly even slightly lower (subcooled water). However, the measured average heat transfer coefficient was consistent with the tests in which the temperature of the upper surface was clearly higher than the extremum temperature. This does not support the assumption that the reason of the discrepancy between results from experiments with and without crust formation would be the density gradient inversion.
2. The ice surface was “rippled” (irregular waves, which at the upper boundary had a height of typically several millimeters or even close to one centimeter). It is possible that the heat transfer behavior is affected by the structure of the ice formation. However, this explanation is not supported by results of BALI experiments, in which the ice layer was smooth but the measured heat transfer coefficients are consistent with COPO II results.

Earlier, the opinion was accepted, that the non-constant fluid properties could be one reason for the unexpected high heat transfer coefficient in experiments with ice formation. But experiments with ice-free boundaries and high temperature difference between pool boundary and the bulk of the fluid showed, that this can not be the reason either.

In stratified pool tests with water, which was heated from the lower side, the upward and sideward Nusselt numbers were determined.

The measured average upward Nusselt numbers from the distilled water layer are well predicted by the Globe and Dropkin correlation [Glo59]:

$$Nu_{up} = 0,069 \cdot Ra^{1/3} \cdot Pr^{0,074}$$

At the side boundary, the measured heat transfer coefficients from the non-heating generating layer are compared to the correlation by Churchill and Chu [Chu75]:

$$Nu_{sd} = \left(0,825 + \frac{0,387 \cdot Ra^{1/6}}{\left(1 + (0,492/Pr)^{9/16}\right)^{8/27}} \right)^2$$

The results and the discussion of the experiments in the COPO-II facilities can be seen in detail in [Hel99].

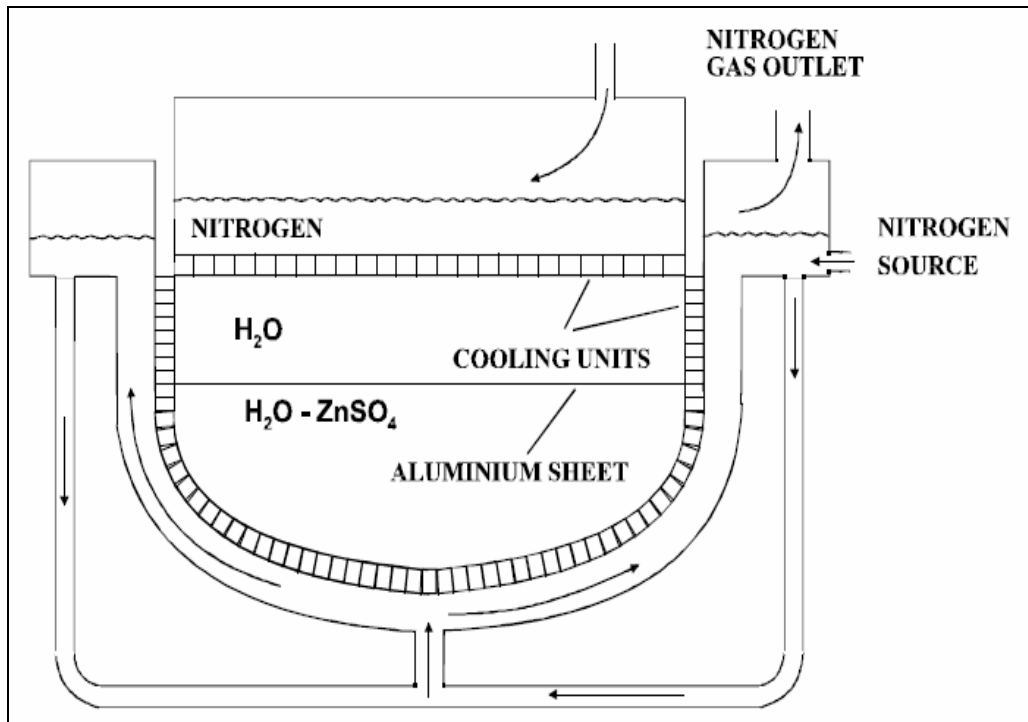


Fig. 3-4: Schematic of the COPO II-Lo facility (from [Hel99])

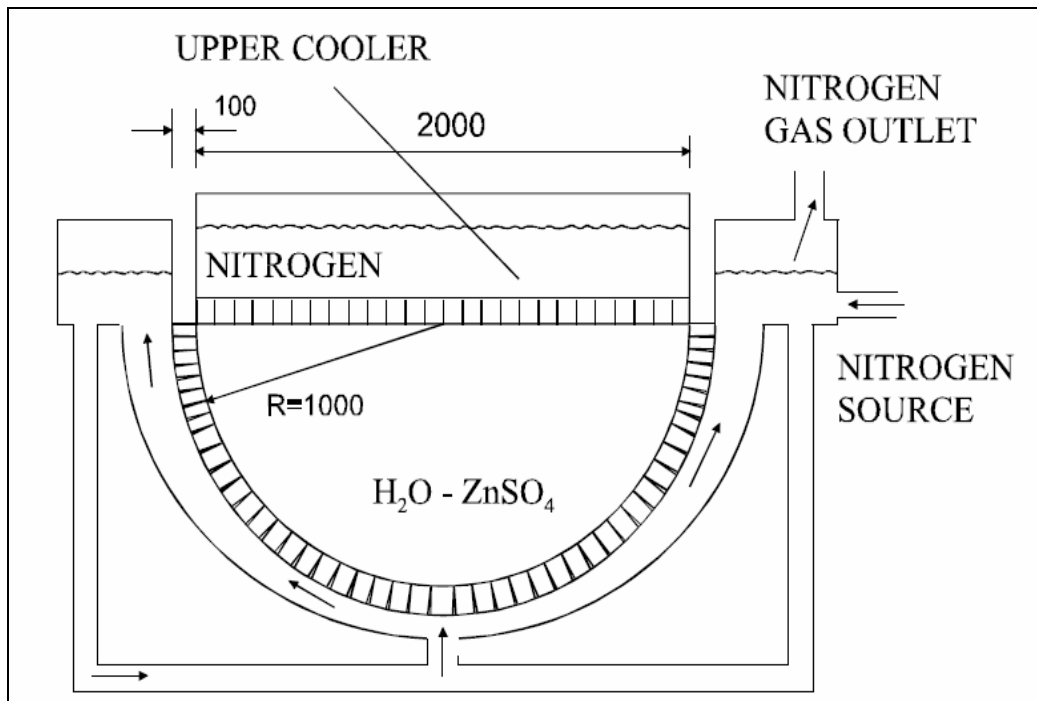


Fig. 3-5: Schematic of the COPO II-AP facility (from [Hel99])

3.2 BALI experiments

The BALI program was designed to study the thermal hydraulics of a corium pool for in-vessel or ex-vessel situation [Ber98]. The experiments were conducted at CEA, France. The corium melt is represented by salted water and the lower head or the core catcher by a 2D-slice at scale 1:1 of constant thickness (15 cm) (see Fig. 3-6). These dimensions provide values of internal Rayleigh numbers of 10^{16} to 10^{17} , for lower head geometry, matching those in the prototypic situation for French PWR.

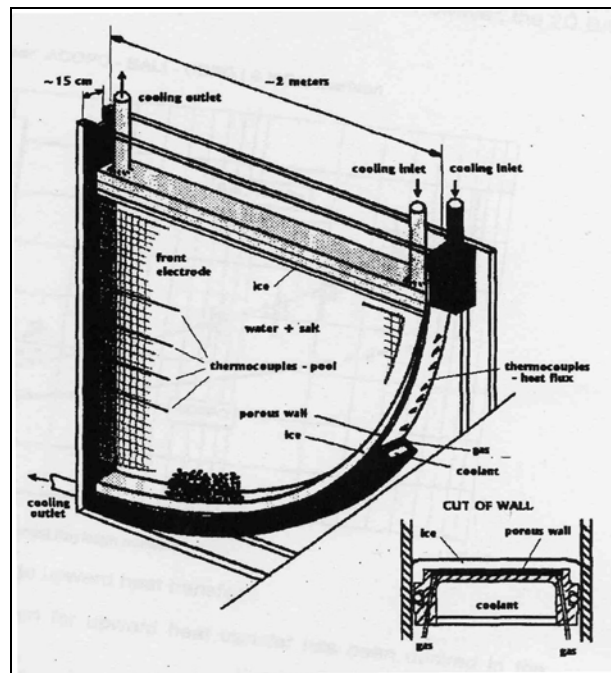


Fig. 3-6: The BALI test section (from [Ber98])

The pool is cooled from the bottom and the top and heated electrically by Joule effect with current supplies located on the sides. The coolant is an organic liquid which may be used within a temperature ranging from $-80\text{ }^{\circ}\text{C}$ to $0\text{ }^{\circ}\text{C}$, thus an ice crust forms at the pool boundaries to provide a constant temperature boundary condition.

The measurements consist of heat flux distributions along the pool boundaries and axial temperature distributions in the pool. Velocity fields may also be measured.

The test matrix includes variations of the water height, power density, water viscosity, pool porosity, cooling conditions and superficial gas velocity.

The following correlations were derived for the upward and downward Nusselt numbers in BALI experiments [Ber98]:

$$Nu_{up} = 0,736 \cdot Ra_i^{0,216}$$

$$Nu_{dn} = 0,123 \cdot \left(\frac{H}{R}\right)^{-0,35} \cdot Ra_i^{0,25}$$

Fig. 3-7 shows the experimental results for the upward heat transfer compared with COPO- and ACOPO results.

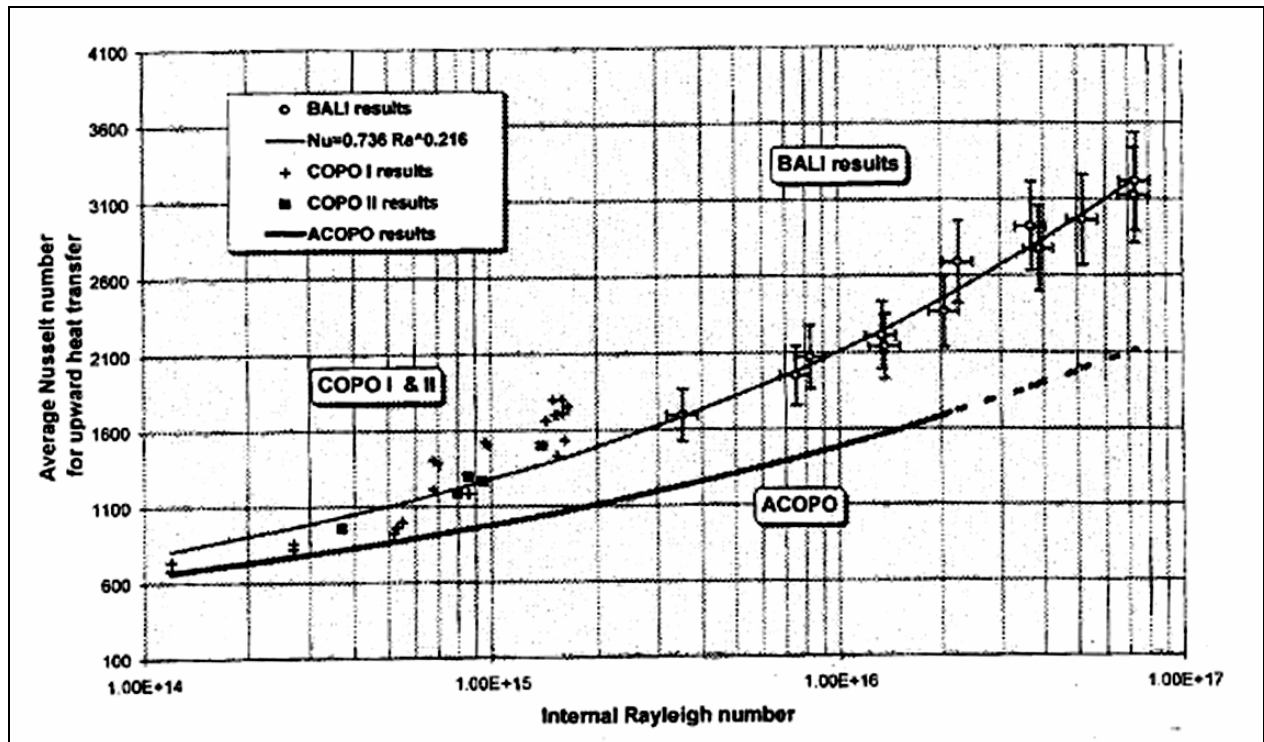


Fig. 3-7: Upward heat transfer ACOPO – BALI - COPO I – COPO II comparison (from [Ber98])

Stratified configuration of the melt was also studied in the BALI metal layer program to address the focusing effect phenomena of a metallic layer at the top of the core melt [Ber98]; [Seh03]. A 2-m-wide, 15-cm-thick 2D rectangular test section was designed and water was employed as simulant fluid. The pool was heated from below to simulate heat flux coming from oxidic pool, cooled on the lateral walls with uniform temperature condition (ice crust formation) and on the upper boundary with a plastic heat exchanger with coolant at 0 °C. The thermal resistance of this plastic exchanger can reproduce the equivalent thermal resistance of a realistic heat transfer, which occurs in the case of radiation.

Different tests have been made for 5 to 40 cm height with uniform or non uniform bottom heat flux (no power injected in the first 40 cm near the cooled wall in case of non uniform heat flux). Fig. 3-8 shows the heat flux concentration factors (ratio between average lateral heat flux to average bottom heat flux) of the metal layer experiments compared with several correlations.

The results of these experiments can be found in detail in [Ber98], [Seh03].

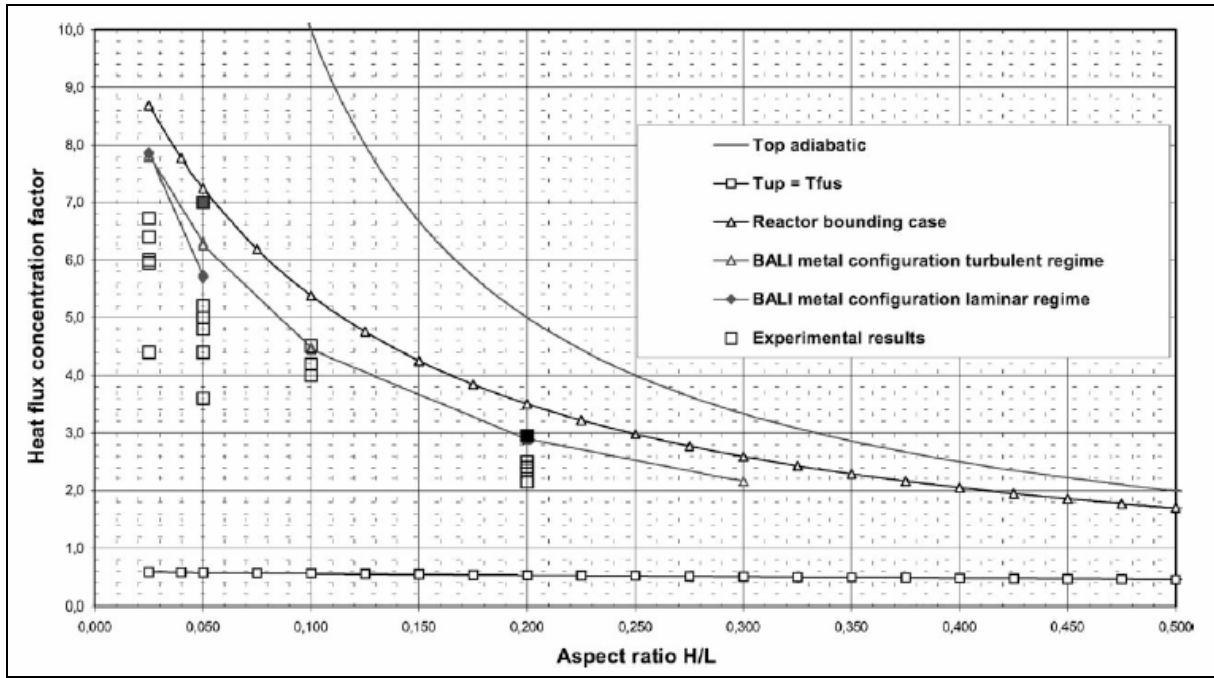


Fig. 3-8: Average lateral heat flux in metal layer experiments of BALI (from [Ber98])

The author of [Ber98] has given neither an explanation for the curves nor a reference to get more information about the other curves. Only the marks “Experimental results” are of interest for us.

3.3 SIMECO experiments

The SIMECO experiments were conducted at KTH in Sweden [Ste05]. SIMECO is also foreseen for experiments in a 2D-geometry. This experimental facility consists of a slice type vessel that includes a semicircular section and a vertical section scaled 1:8 of prototype PWR type reactors. This represents the lower head of the reactor vessel. A cable type heater with 3 mm in diameter and 4 m in length provides internal heating of the melt pool in the lower head. The brass wall which models the RPV wall is externally cooled by a controlled water loop. On the top of the vessel a heat exchanger with regulated water loops is employed to measure the upward heat transfer. The schematic of SIMECO is given in Fig. 3-9

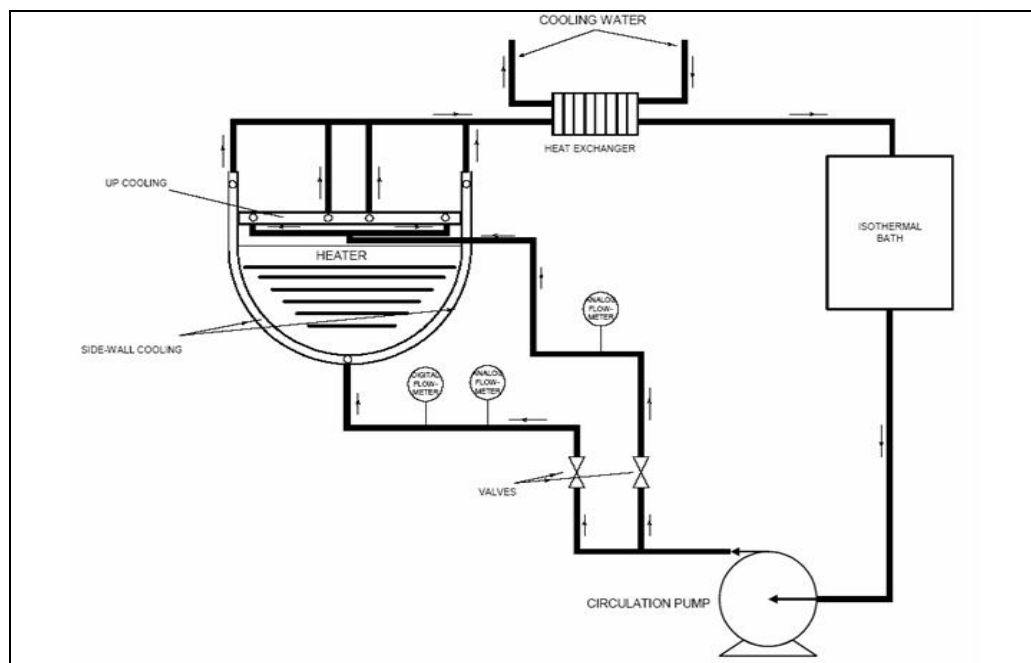


Fig. 3-9: Schematic of the SIMECO facility (from [Ste05])

The sideways and upward heat fluxes are measured by employing arrays of thermocouples at several different angular positions. A total of 64 K-type thermocouples are mounted to obtain data on sidewall heat flux, heat flux on top of pool, inlet and outlet water temperatures, as well as pool temperatures inside the vessel, and the upper heat exchanger. The location of the thermocouples is given in Fig. 3-10.

Practically isothermal boundary conditions are provided at vessel boundaries with help of an isothermal bath. A plate type heat exchanger was mounted in the isothermal bath circuit to increase the cooling capacity of the isothermal bath. The cooling circuit has two parallel paths, one for sidewall heat exchange and another for top heat exchange. Top heat exchanger flow is established by an isothermal bath inbuilt recirculation pump. A second external recirculation pump was mounted in order to establish the necessary flow rate for the sidewall heat exchanger. A digital flow meter measures top heat exchange flow [Seh04a], [Ste05].

The diameter and height of the test section are respectively 62.0 cm and 53.0 cm. The width of the slice is 9.0 cm. The front and back faces of the facility are insulated in order to prevent

heat loss. The vessel wall has a thickness of 2.3 cm. (for the main dimensions see Fig. 3-11).

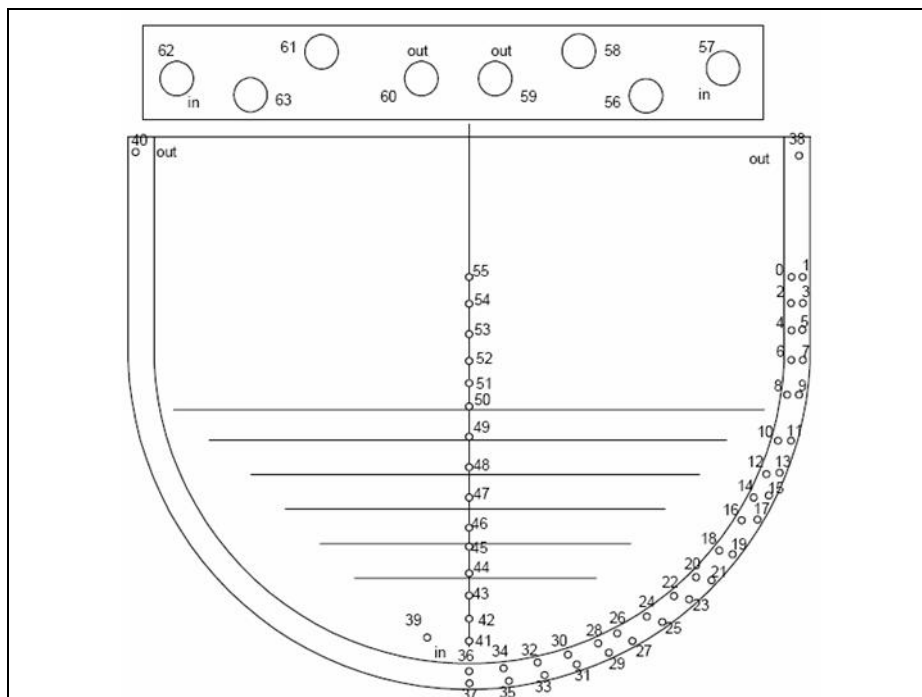


Fig. 3-10: Location of the thermocouples in the SIMECO facility (from [Ste05])

Two-layer experiments are described in more detail in [The00]. The experiments were conducted with a liquid mixture from Benzyl benzoate (BBO) and Parafin oil (PO), whose phase diagram shows a temperature dependent miscibility gap. Fig. 3-12 shows this miscibility gap as function of temperature. For a given weight fraction of PO at a temperature below the curve (only points from experiments shown) the liquids are separated and above the curve the liquids form a mixture.

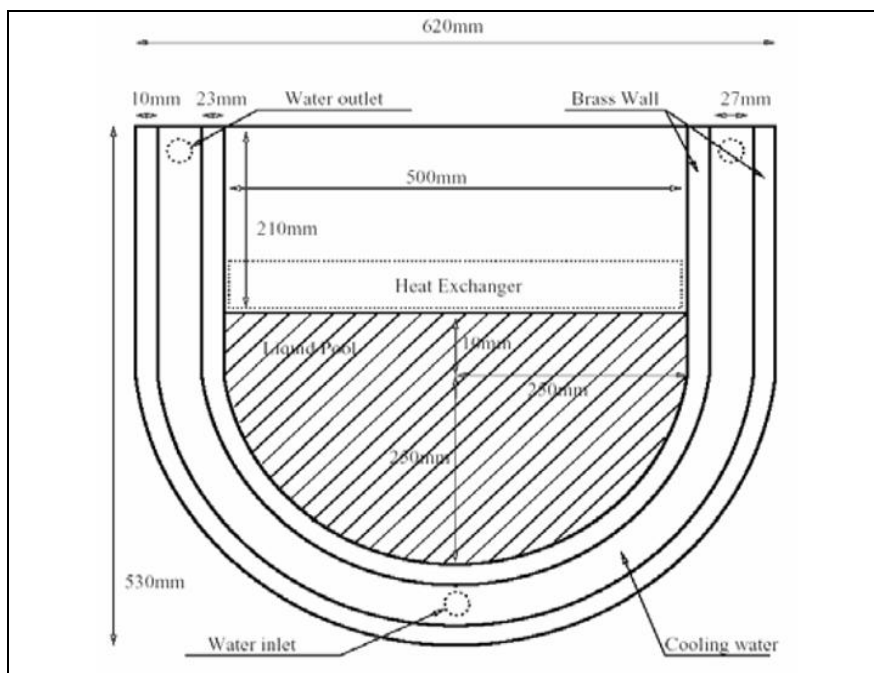


Fig. 3-11: Main dimensions of the SIMECO vessel (from [Ste05])

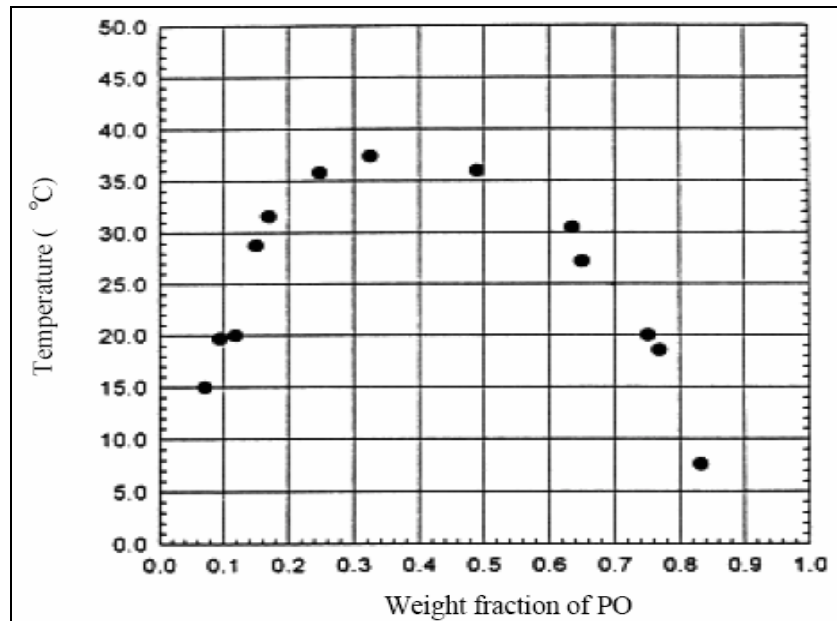


Fig. 3-12: Miscibility gap for the mixture of Benzyl benzoate and Paraffin oil (from [The00])

In one series of experiments the components were mixed at a temperature above their phase separation temperature and then poured into the facility. The results of these experiments were compared with results in a uniform water pool.

Another series of experiments was conducted, in which the initial condition is that of a separated layer pool. In these experiments the mixing process could be studied. These experiments showed that the temperature at the top of the pool decreases during the mixing process (Fig. 3-13).

In the three-layer experiments paraffin oil, water and chlorbenzene (1106 kg/m^3) were employed to investigate stratification of three immiscible fluids. The height of the lower pool (chlorbenzene) was between 4 and 7 cm, the thickness of the middle layer (water) was between 15 and 20 cm and the upper layer (paraffin oil) was between 3 and 7 cm. The total height of all layers in all experiments was constant 27 cm. The Rayleigh number was found to be in the same range as in the experiments with two layers (from $6.01 \cdot 10^{12}$ to $8.7 \cdot 10^{12}$).

More detailed information about the heights of the layers and the distribution of the heat in three-layer experiments is given in [Seh04b].

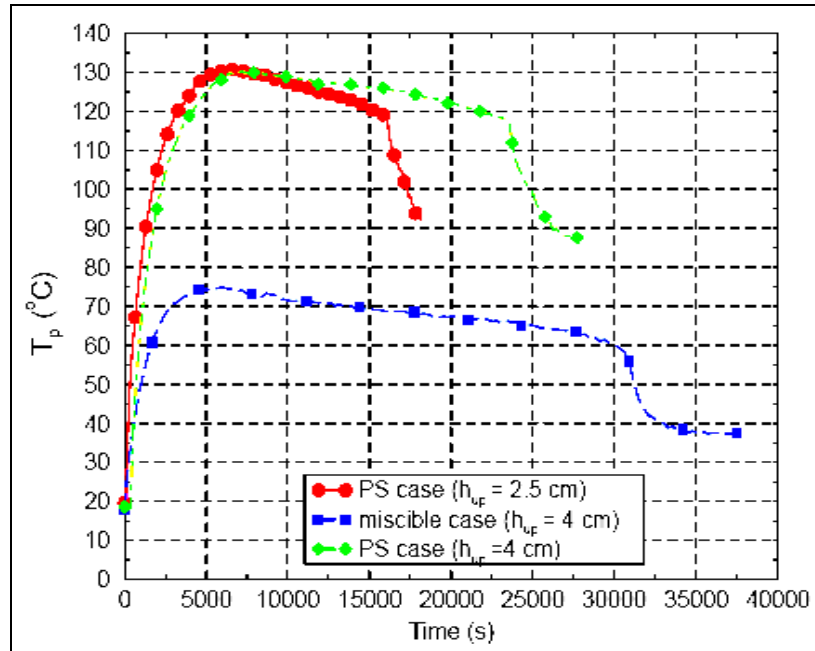


Fig. 3-13: Transient during the mixing process (thermocouple near the top of the pool), (from [The00])

3.4 ACOPO experiments

The ACOPO test section is a hemispherical container with a diameter of 1.83 m (72 inch). The boundary of the vessel can be kept to a desired temperature by circulating the contents of a large water bath. A segmented structure of the boundary, as shown in Fig. 3-14, allows the determination of local heat fluxes.

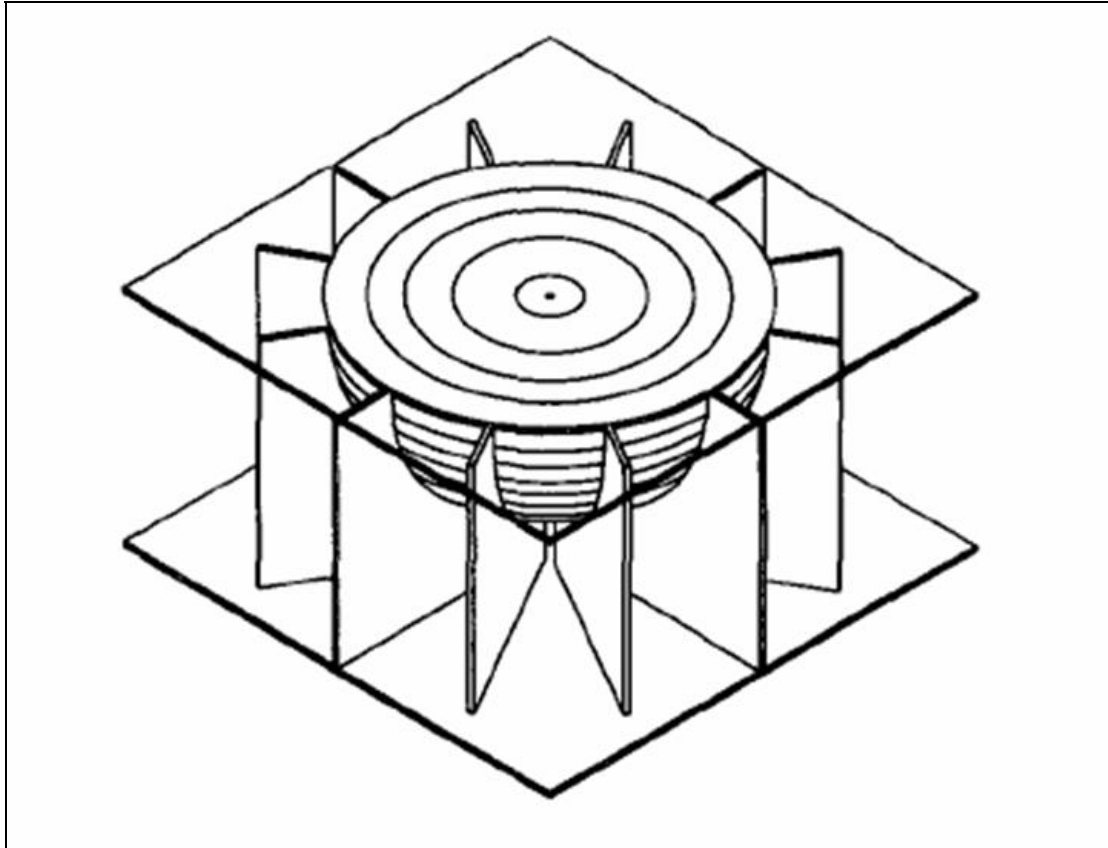


Fig. 3-14: Schematic of the ACOPO test vessel with individual cooling unit (from [The97])

The segments are called 'cooling units', and there is a total of 15 of them, ten around the hemispherical boundary and five above the lid. The positions of the thermocouple positions can be taken from Fig. 3-15.

Each cooling unit is independently fed by a respective pump, whose speed is controlled. The schedule of the ACOPO facility is shown in Fig. 3-16.

In the ACOPO experiments there is no internal heat source. The fluid is preheated to some high initial temperature and then poured into the vessel. The idea behind this approach is to simulate volumetric heating, by suddenly cooling the boundaries and interpreting the transient system cool-down as a sequence of quasi-stationary natural convection states. Theofanous et al. wrote in [The97]: "...by using the internal energy of the fluid, preheated to some high initial temperature, to simulate volumetric heating, by suddenly cooling the boundaries and interpreting the transient system cool down as sequence of quasi-stationary natural convection states. That is, from the local instantaneous fluxes at the boundaries, a total heat loss rate can be obtained to define the instantaneous Rayleigh numbers, which then are correlated to the instantaneous Nusselt numbers. The idea is that the cool-down would be ar-

rested, and nothing would really change, if at any instant at time during the cool down, a volumetric heating rate could be supplied that was equal to the heat loss rate”.

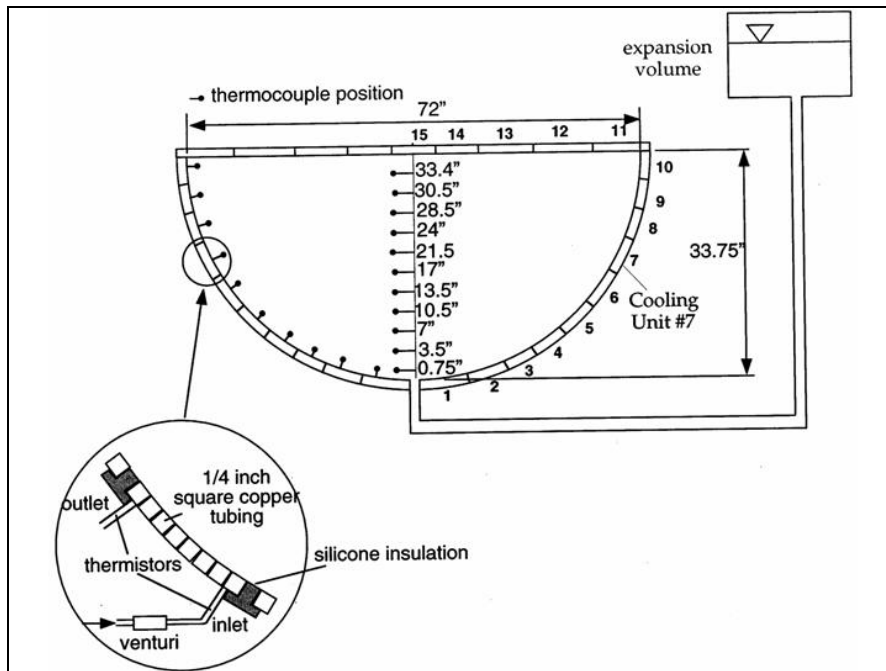


Fig. 3-15: Key construction details and instrumentation (from [The01])

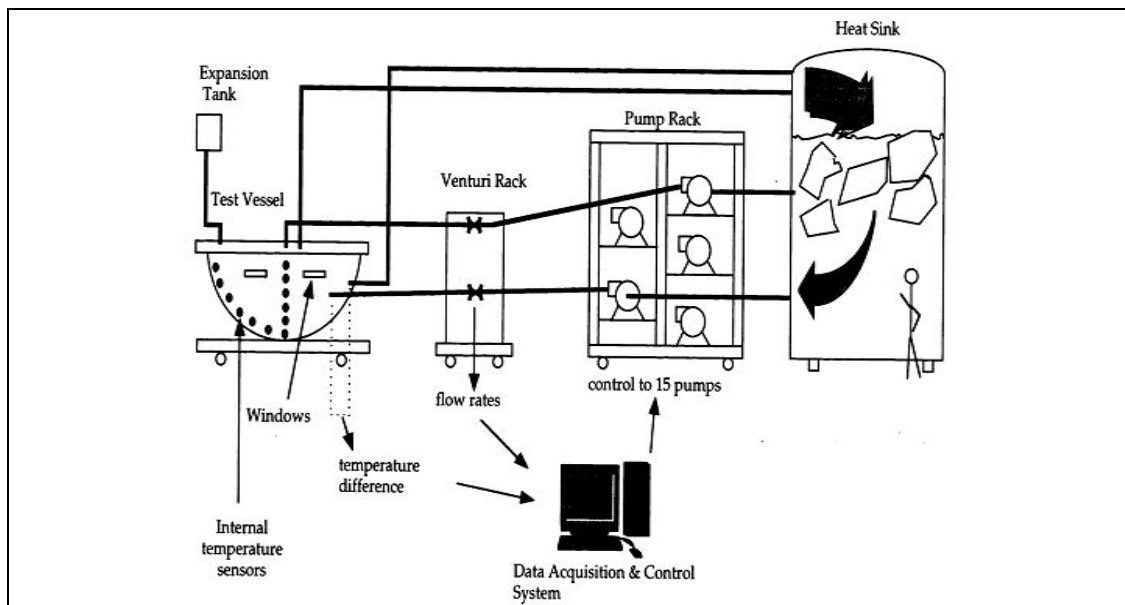


Fig. 3-16: Schematic of the ACOPO experiment (from [The01])

However the ACOPO approach has some important limitations. The reason is that the cool-down of a fluid without internal heat sources (as in the ACOPO experiments) is governed by a differential equation different from that for the steady state solution of a fluid with internal heat sources. The energy conservation equation in the steady state case is:

$$\nabla \cdot (\rho c UT - k \nabla T) = Q_v$$

The right side of this equation is zero in experiments without internal heat generation (like in the ACOPO experiment). In the case, when internal heat sources are present in the melt, the right side is greater than zero, and this should lead to a completely different temperature- and velocity field. Indeed the total heat loss rate could be maintained, and nothing would really change, if at any instant at time during the cool down, a volumetric heating rate could be supplied that was equal to the heat loss rate at the boundaries. But the spatial distribution of these required heat sources is certainly not the same as in experiments with internal heat sources. That means that identical boundary conditions at any instant result in different temperature fields in each case. An indication of that gives the diagram in Fig. 3-17, which compares ACOPO-results with the Steinberner-Reineke correlation.

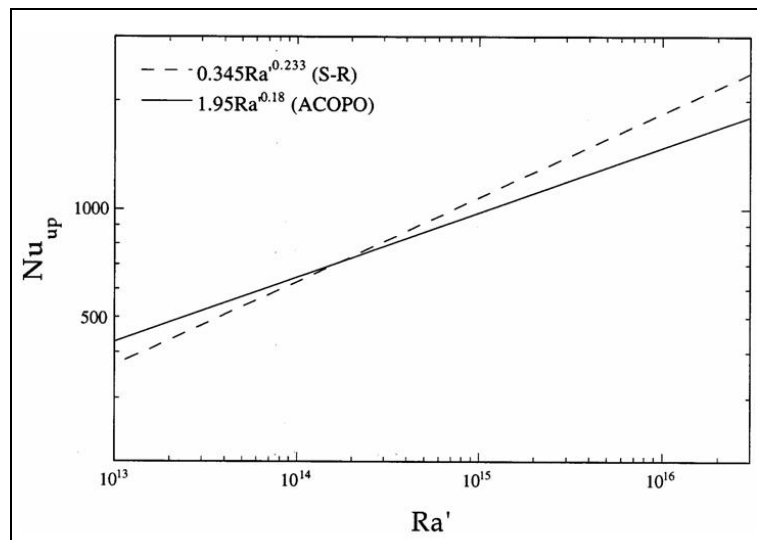


Fig. 3-17: Upward heat transfer from ACOPO compared to the Steinberner-Reineke correlation (from [The01])

The Steinberner-Reineke correlation provides higher Nusselt numbers especially for high Rayleigh numbers. That is not surprising, because the heat sources drive the hot mass elements faster to the upper boundary in the middle of the pool. This in turn leads to higher Nusselt numbers. We refer also to page 6, where was elaborated on, that the Steinberner-Reineke correlation was originally limited to $Ra=10^7$ (see Fig. 3-3).

But it might be interesting to investigate this approach experimentally. The LIVE facility gives the possibility to compare experiments with and without internal heat sources.

3.5 RASPLAV experiments

The experiments in the frame of the international RASPLAV project were conducted at the Kurchatov Institute in Russia. These experiments covered investigations in several facilities with prototypic materials (corium) and with NaF-NaBF₄ mixtures (salt). All experiments were conducted in slices similar to SIMECO and BALI experiments.

Only the salt experiments will be described in this report, because the experiments with other materials are not relevant for the LIVE program.

Detailed information about the project is given in [Asm00]

Fig. 3-18 shows the geometry of the lower plenum-model in RASPLAV.

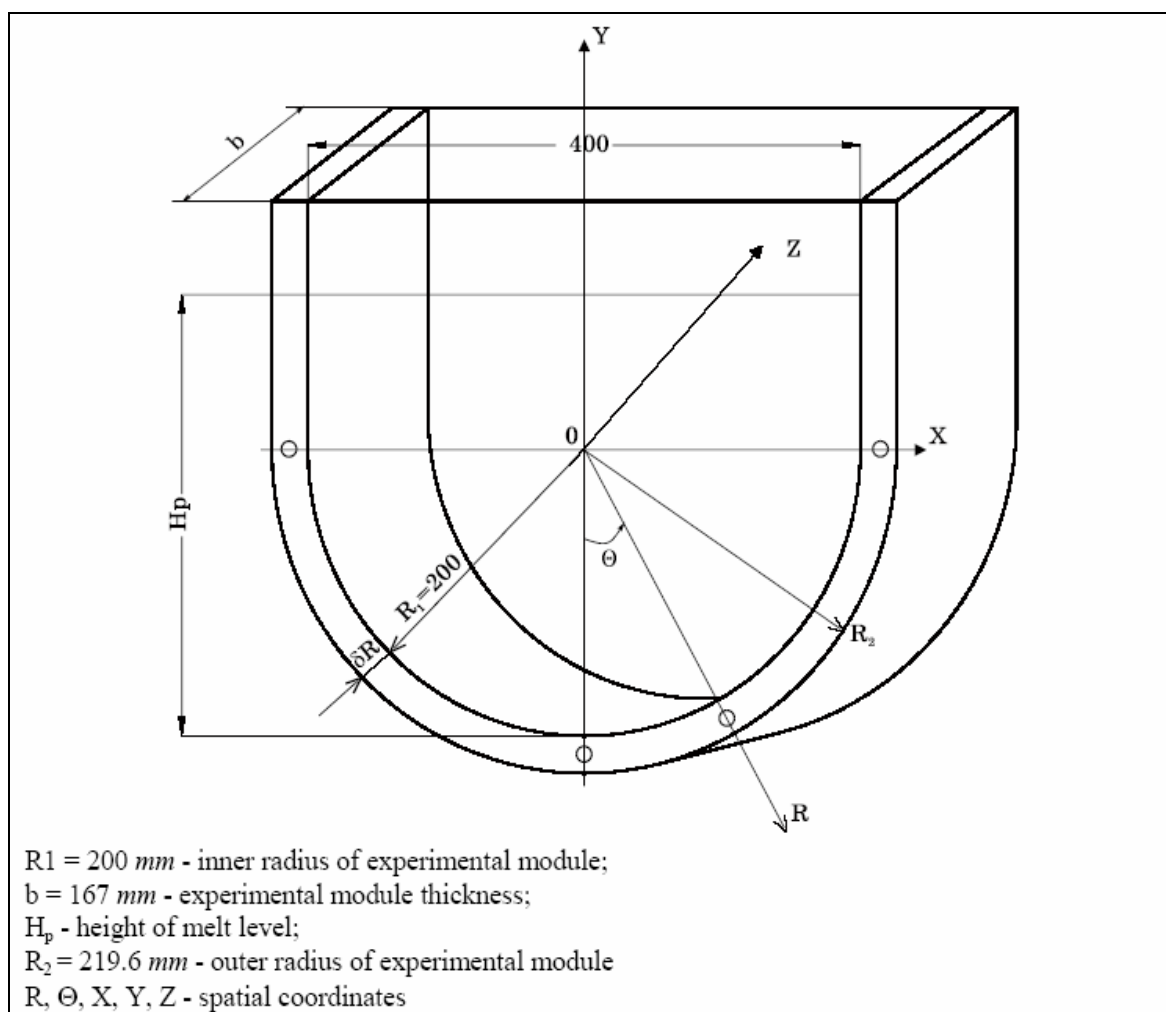


Fig. 3-18: System of coordinates adapted in RASPLAV-A-salt experiments (from [Asm98b])

Fig. 3-19 shows the layout of the thermocouples in the melt pool.

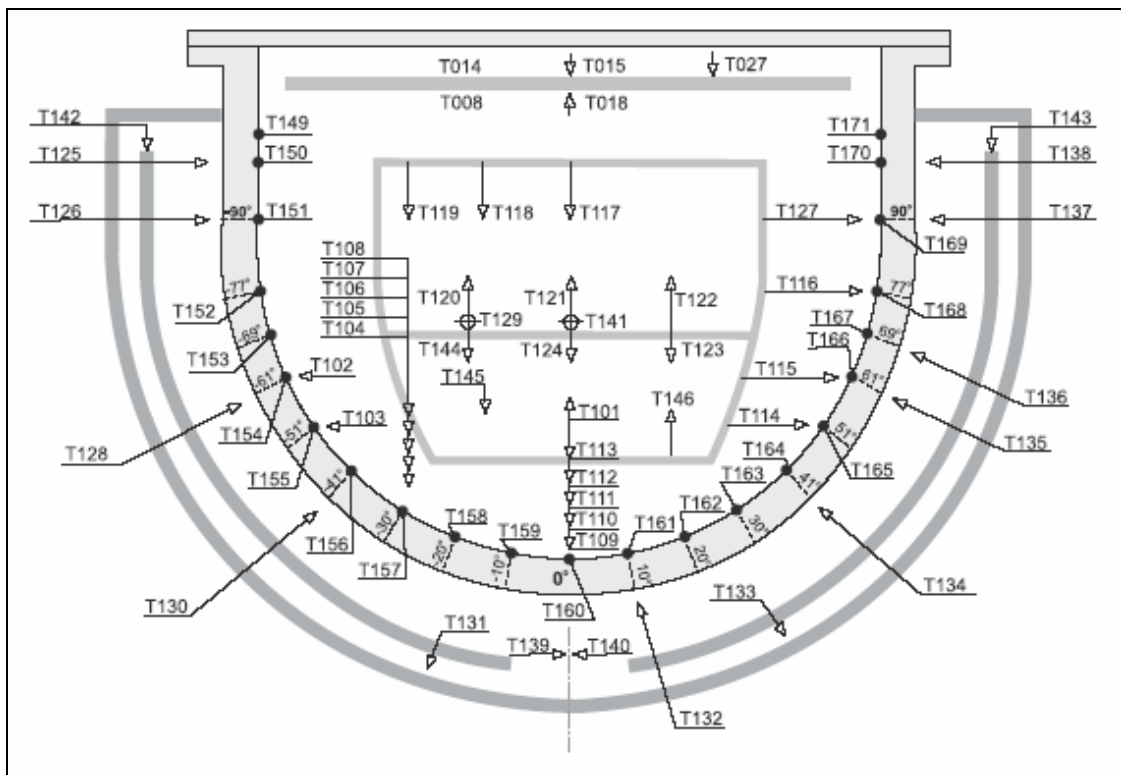


Fig. 3-19: Layout of the thermocouples in the melt pool (from [Asm98b])

The first run of the salt facility was completed in May 1996 during which 19 steady-state convection regimes of $8\text{NaF}-92\text{NaBF}_4$ melt were studied. A distinguishing feature of this series resides in the fact that it was conducted under non-isothermal boundary conditions on the outer cooled wall at the use of side wall heating method (SWH). Such boundary conditions were not prototypic for the reactor case when the vessel is cooled in emergency conditions by water boiling on the outer surface. Nevertheless, the results of this run are of certain interest. In this series of experiments the attempts failed to obtain regimes of melt convection with crust formation over the entire inner surface of the vessel model, the crust grew only in the range of the angle coordinates from -61° to $+61^\circ$.

The second series of salt experiments was conducted in September 1996. The SWH method was used in this run and boundary conditions at the top surface of the pool were nearly adiabatic. The external coolant was realized by a melt of $\text{NaNO}_2 - \text{NaNO}_3 - \text{KNO}_3$ salt. In this series maximum temperature of $8\text{NaF} - 92\text{NaBF}_4$ melt varied from 408°C to 609°C for different regimes. The effective density of the heat generation was $q_v = 0.78 \cdot 10^5 - 6.09 \cdot 10^5 \text{ W/m}^3$ which corresponded to the values of $\text{Ra}' = 4.7 \cdot 10^{11} - 1.61 \cdot 10^{13}$ and $\text{Pr} = 4.56 - 7.74$.

The third series of salt experiments was conducted in April 1997 with the objective to investigate heat transfer in a volumetrically heated pool. For this purpose the facility was upgraded by the implementation of the direct electric heating (DEH) method. The inner surface of the melt bath (vessel model) was coated by a specially developed insulating composition which contained oxides of zirconium, chromium and lanthanum, using the method of laser sputtering. The coating was in contact with the melt for 60 hours and ensured the conditions of

nearly constant density of power deposition over the entire volume of the melt pool (q_v almost const) throughout this series of experiments. 9 steady state regimes of convection in 8NaF - 92NaBF₄ melt were realized in this run with an average density of power deposition range from $8.1 \cdot 10^4$ to $3.3 \cdot 10^5$ W/m³ and temperature range from 408 °C to 588 °C. The crust was produced over the entire inner surface of the test wall in 3 regimes. As planned, the run of salt tests was conducted in the same region of characteristic parameters and under identical boundary conditions as in the second run utilizing SWH method. It allows to compare the obtained data and to answer the question of an impact of heating techniques (SWH and DEH) on heat transfer in corium. In the third series of salt experiments the values of characteristic numbers ranged within the following limits: for Rayleigh number $Ra' = 2.7 \cdot 10^{11} - 1.36 \cdot 10^{13}$ and for Prandtl number $Pr = 5.07 - 7.73$. The radiation heat flux from the melt surface did not exceed 17 % in a majority of regimes.

The fourth series of experiments was conducted utilizing a binary non-eutectic composition of 25NaF - 75NaBF₄ salts with a big difference between the solidus and liquidus temperatures ($T_{sol} = 384$ °C, $T_{liq} = 610$ °C). The objective of this run was to investigate heat transfer due to natural circulation in case of the existence of a mushy zone. Studies were conducted in a wide range of maximum melt temperature from 454 °C to 708 °C. In order to avoid the crystallization of the low melting NaBF₄ component the wall temperature was maintained above its liquidus temperature ($T_w > 408$ °C) in all regimes. 10 steady state heat transfer regimes were realized in this series of experiments and, two of those regimes were realized for a purely liquid phase of the melt in the pool when melt temperature exceeded T_{liq} over the entire volume. The remaining regimes had the crust and mushy zone at the boundary of heat exchange near the wall.

Major findings of these experiments were:

3. At first the crust is formed at the bottom part of the pool with the $\Theta = 0$ coordinate where temperature always remains minimal. The crust thickness adjusts itself according to the distribution of the heat flux and varies insignificantly as function of the Θ angle. The relative crust thickness along the vessel wall normalized to its maximum value at $\Theta = 0$, is fitted satisfactorily (with ± 25 % deviation) by the following equations:

$$\frac{d(\Theta)}{d(0)} = 1 - 4,44 \cdot 10^{-2} \Theta + 2,22 \cdot 10^{-3} \Theta^2 - 3,65 \cdot 10^{-5} \Theta^3 \quad \text{for } 0 \leq \Theta < 41^\circ$$

and

$$\frac{d(\Theta)}{d(0)} = 1,57 - 3,88 \cdot 10^{-2} \Theta + 2,43 \cdot 10^{-4} \Theta^2 \quad \text{for } 41 < \Theta \leq 41^\circ$$

4. The presence of a crust along the cooled test wall does not change significantly the average downward heat transfer. The experimental data confirm the similarity of heat transfer.
5. The experiments with the 25NaF - 75NaBF₄ non-eutectic composition, which is characterised by a wide temperature range between solidus and liquidus, show that thermal characteristics in the temperature region above T_{liq} do not differ from those which were obtained with the 8NaF - 92NaBF₄ eutectic melt composition in the second series of salt experiments. However, a difference is observed in the temperature distribution in the temperature region $T_{sol} < T_p < T_{liq}$. The local heat

flux distribution is rather similar to that obtained for regimes with and without crust but differs from both ones.

6. The transition from slice to hemispherical geometry was made based on the assumption of identity of heat transfer for both cases. The similarity of heat transfer processes was confirmed by comparison of local and integral data which were obtained in the slice model with the corresponding results of Mini-COPO and UCLA experiments in a hemispherical geometry. For hemispherical geometry the heat transfer equation derived using salt test data and calculated form factor for volumetrically heated pools can be written in the following form:

- For the average heat transfer:

$$Nu_{dn} = 0,138Ra^{0,242}$$

- For the ratio of Nusselt Number at angle Θ to the average Nusselt Number:

$$\frac{Nu(\Theta)}{Nu_{dn}} = 0,165 + 1,55 \cdot 10^{-2} \Theta - 7,68 \cdot 10^{-4} \Theta^2 + 1,87 \cdot 10^{-5} \Theta^3 - 1,09 \cdot 10^{-7} \Theta^4$$

Fig. 3-20 illustrates the second correlation.

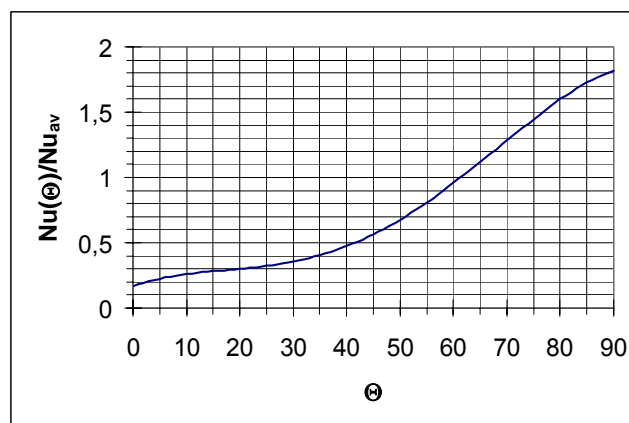


Fig. 3-20: Ratio of Nusselt number at angle Θ to the average Nusselt number

An extended presentation of the results of salt experiments is given in [Asm98b].

4 SURVEY OF KEY PROBLEMS CONCERNING THE CORE MELT IN THE LOWER PLENUM

Asmolov et al. gave a comprehensive survey of the phenomena associated with the In-Vessel Retention issue in 2001 [Asm01]. We give here the table of the phenomena associated with the in-vessel retention from this literature.

Table 4-1: Phenomena associated with In-Vessel Retention issue (from [Asm01])

Phenomena	Experimental programs	Knowledge base
1. Decay heat and fission products		
1.1 Residual heat level		Reasonable
1.2 Partitioning of the decay heat between layers in case of stratified pools	Under discussion	Limited
1.3 FP and residual heat distribution between crust and pool	Under discussion	Limited
1.4 FP release from molten pool		Limited
2. Melt thermal hydraulics		
2.1 Single phase liquid pool	COPO, ACOPO, BALI, RASPLAV, SIMECO	Good
2.2 Complex mixtures	RASPLAV salt, SIMECO	Limited
2.3 Stratified liquid pools	SIMECO	Limited
2.4 Oxidic and metallic pools (focusing effect)	Planned SIMECO, RASPLAV-salt, COPO, BALI	Reasonable
2.5 Effect of crust formation on heat transfer	COPO, BALI, SIMECO, RASPLAV	Reasonable

continued on next page

Phenomena	Experimental programs	Knowledge base
3. Heat flux removal		
3.1 Gap formation and heat transfer	CTF (see [And89]), FOREVER (see [Seh99]), SONATA (see [Kim98])	Limited
3.2 Boiling on downward curved surfaces	UCSB, Penn St., SULTAN	Good
3.3 Debris bed dryout and coolability	POMECO (see [Yan99])	Reasonable
3.4 Radiation from the upper surface		Reasonable
3.5 Melt relocation scenarios		
3.6 Formation of the initial molten pool in the core	CORA (see [Hof94]) PHEBUS-FP (see [Sch99])	Reasonable
3.7 Melt pool growth and pathway of melt relocation to the lower head	PHEBUS-FP	Limited, depends on In-vessel-design
3.8 Melt composition		Limited
3.9 Additives: FeO, B ₄ C, etc.	Phebus-FP, CORA	Limited
3.10 Interaction with structures	MP-tests	Limited
4. Melt composition and chemistry		
4.1 Mass of metallic and oxidic components		Limited
4.2 Chemistry in liquid phase (melt stratification)	RASPLAV	Limited
4.3 Hypostoichiometric oxides and metallic U behavior	RASPLAV	Limited

continued on next page

Phenomena	Experimental programs	Knowledge base
4.4 Crust formation	RASPLAV	Limited
4.5 Intermetallic reactions	RASPLAV, planned	Limited
4.6 Corium properties (UO ₂ -Zr-ZrO ₂)	RASPLAV	Reasonable
5 Vessel failure modes		
5.1 Vessel breach, high pressure	LHF (Sandia) (see [Chu99])	Reasonable
5.2 Creep simulation and low pressure breach	OLHF (see [Meg99]) FOREVER	
5.3 Irradiated vessel		
5.4 Vessel impingement	MVI project (see [Seh99])	Reasonable
6. Transient processes		
6.1 Jet formation		
6.2 Steam explosion	FARO (see [Meg99]) KROTOS (see [Huh99])	Limited
6.3 Fragmentation		
6.4 Dynamic loads		Reasonable
6.5 Vessel breach		Limited

Recently the priority assessment of the phenomena related to the late phase was done in the SARP (Severe Accident Research Priorities) work package in the frame of SARNET. The objective of SARP is to provide the Governing Board of SARNET with guidelines for defining the orientations to be given to the Joint Program Activities (JPA) in terms of joint activities for research of common interest and high priority. This includes reassessing the priorities for research to be performed in the field of severe accident phenomena and management. The EURSAFE issues and their revised priority are given in Appendix B.

The LIVE experiments will focus on all sub-issues of issue 2 (Melt thermal hydraulics) in Table 4-1. A survey of phenomena to be investigated in the LIVE facility will be given in chapter 5.3. There and in chapter 5.4 the relationship between the single issues in Table 4-1 and the LIVE program is explained in more detail.

We continue with a detailed description of the LIVE facility and the simulant materials in the next two chapters.

5 The LIVE TEST FACILITY TO INVESTIGATE MELT BEHAVIOR IN THE RPV LOWER HEAD

5.1 Description of the LIVE test facility

The LIVE experimental facility is designed to study the late phase of core degradation, onset of melting and the formation and stability of melt pools in the RPV. Additionally, the regaining of cooling and melt stabilization in the RPV by flooding the outer RPV or by internal water supply will be investigated. Steady state behavior of debris and of molten pools in the lower head has been already investigated in several experimental studies. However, the database for the transient processes during core melting, melt relocation and accumulation is still very limited. For the melt released into the lower head of the vessel, there is a lack of information about e.g. transient heat fluxes to the vessel wall, crust formation, stability and re-melting of melt crusts, as may occur from melt release to steady state and under 3D geometrical situations. An improved understanding of these processes can help to define accident management procedures for accident control in present reactors.

The LIVE program is divided into three different phases. In the first phase (LIVE1) the investigations will concentrate on the behavior of a molten pool, as it is poured into the lower head of the RPV, and take into account transient and possible 3D effects (Fig. 5-1). The melt pool can consist of an oxide melt or both oxide and metal melts to simulate the components of a real corium melt. The melt masses and the conditions outside the test vessel can be varied to simulate different accident scenarios. Important phenomena, which are investigated, are:

- time dependent local heat flux distribution to the lower head,
- possible crust formation of the melt depending on the power density and the external cooling modes,
- gap formation between the RPV wall and the melt crust,
- effect of phase segregation of a non-eutectic melt on the solidification behavior.

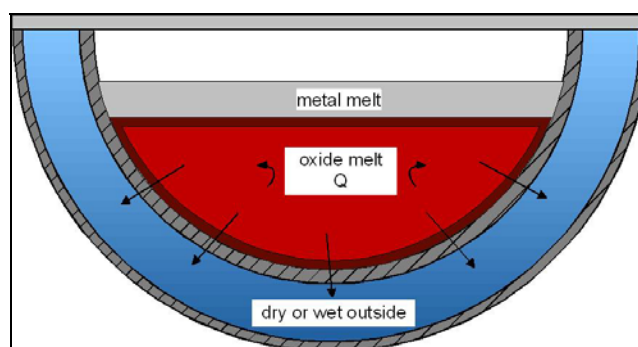


Fig. 5-1: Melt retention in the lower head (LIVE1)

In LIVE2, pool formation and behavior will be studied under the conditions of multiple pours of melt from the core region. The presence of water in the lower vessel head is an option for further studies (Fig. 5-2). The simulant melt can be pure oxidic or can be an oxide melt and a metal melt. The melt release can be in subsequent pours and at different positions (central and/or non-central). The phenomena, which will be investigated, are similar to LIVE1.

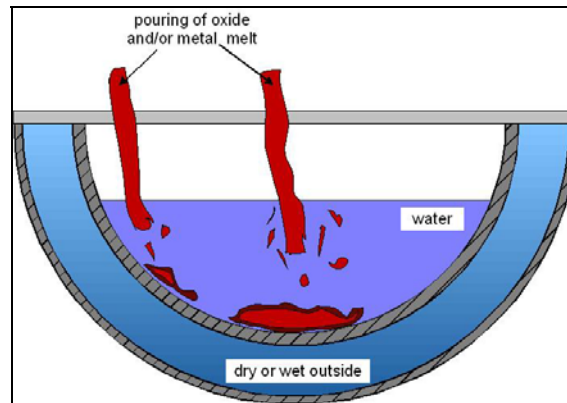


Fig. 5-2: Melt relocation to the lower head (LIVE2)

The third phase (LIVE3) will start with a simulated in-core corium pool. Main emphasis is on the stability of such melt pools during different cooling modes and subsequent relocation processes at crust failure.

Important phenomena to be investigated are crust growth around the pool, stability and failure modes of the crust, the release rates and flow paths of the melt from the in-core melt pool, the accumulation of the released melt in the lower head and its coolability and finally necessary conditions to stabilize the melt pool in the core region.



Fig. 5-3: LIVE test vessel (from [Fzk08])

Core of the LIVE test facility is a 1:5 scaled RPV of a typical pressurized water reactor (Fig. 5-3). For the first and second phase of the experiments (LIVE1 and LIVE2), only the hemispherical bottom of the RPV will be used. The inner diameter of the test vessel is 1 m and the wall thickness is 25 mm. The material of the test vessel is stainless steel. To investigate the transient as well as the steady state behavior of the simulated core melt, an extensive instrumentation of the test vessel is realized (Fig. 5-4).

The vessel wall is equipped with 17 instrumented plugs (Fig. 5-5) at different positions along 4 axes. Each plug consists of a heat flux sensor and 5 thermocouples. The thermocouples are protruding into the melt with different distances from the vessel wall (0, 5, 10, 15, 20 mm). The heat flux sensor is part of the vessel. It is covered by a 1-mm-thick steel plate at the inside of the vessel. This sensor measures the heat flux and the corresponding temperature. To measure the temperature at the outer surface of the vessel wall, 17 thermocouples

are located at different positions along 4 axes. In addition to the 85 thermocouples of the plugs, it is possible to place up to 80 thermocouples in the melt to measure the temperatures of the melt and the crust growth.

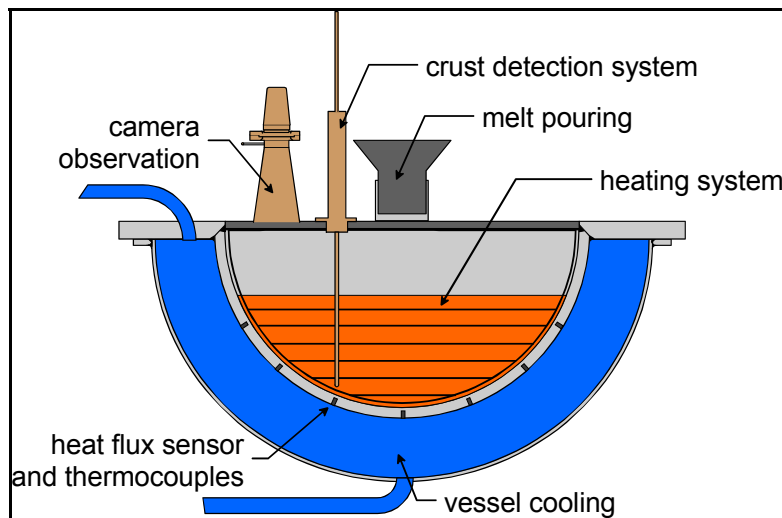


Fig. 5-4: Scheme of the LIVE test facility (from [Fzk08])

The instrumentation of the test vessel includes also an infrared camera and a video camera to observe the melt surface, weighing cells to detect quantitatively the melt relocation process, and mechanical sensors to measure the melt crust thickness at the wall.

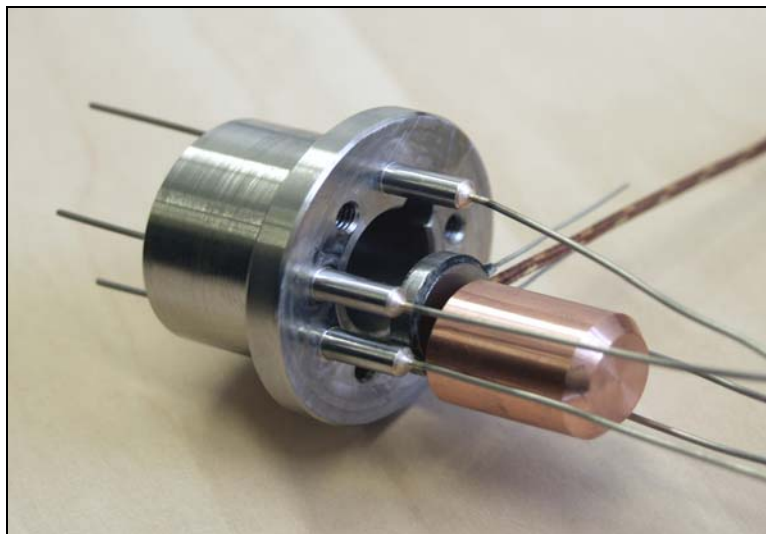


Fig. 5-5: LIVE instrumentation plug (from [Mia07])

The power input into the melt is recorded and melt samples are extracted during the tests. Different openings in the upper lid of the test vessel allow pouring of the melt to the central region or close to the perimeter of the lower head. To be able to investigate the crusts, which are formed at the wall of the vessel, the residual melt is sucked out of the vessel at the end of the test.

To investigate the influence of different external cooling conditions on the melt pool behavior, the test vessel is enclosed by a second vessel (cooling vessel) to be able to cool the test

vessel at the outside by a cooling medium. The cooling medium is introduced at the bottom of the cooling vessel and leaves the vessel at the top.

The volumetric heating system (Fig. 5-6) has to simulate the decay heat released from the corium melt. Consequently, the heating system has to produce the heat in the simulant melt as homogeneously as possible. Therefore a heater grid with several independent heating elements was constructed. The heating elements are shrouded electrical resistance wires. The maximum temperature of the heating system is 1100 °C. The heating system consists of 6 heating planes at different elevations with a distance of about 45 mm. Each heating plane consists of a spirally formed heating element with a distance of ~40 mm between each winding. The heating elements are located in a special cage to ensure the correct position. All heating planes together can provide a power of about 18 kW. To realize a homogeneous heating of the melt, each plane can be controlled separately.

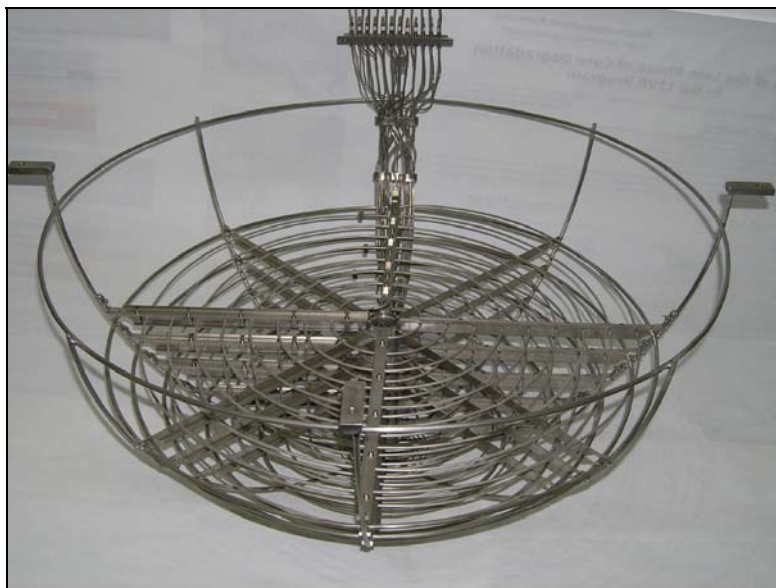


Fig. 5-6: LIVE volumetric heating system (from [Mia07])

To allow transient pouring of the melt into the test vessel, the melt is produced in a separate heating furnace (Fig. 5-7). The capability of this tilting furnace is 220 l volume. Therefore it is possible to produce the total amount of the scaled oxide melt mass and additionally the total amount of the scaled metallic part of the simulated corium melt. The maximum temperature of the heating furnace is 1100 °C. When the melt has reached the desired pouring temperature, the furnace is tilted and the melt is discharged with a specified pouring rate into the test vessel via a heated pouring spout. In addition, the heating furnace is equipped with a vacuum pump; so it is possible to suck the residual melt out of the test vessel back into the heating furnace.



Fig. 5-7: LIVE heating furnace

In summary the LIVE facility has the following features:

- 1:5 scale of the lower head of a prototypic pressurized water reactor,
- 3-dimensional geometry,
- furnace to heat up the melt before the pouring of the melt,
- different openings in the upper lid to pour the melt at different positions into the vessel,
- volumetric heating of the simulant melt,
- 17 instrumented plugs at the vessel wall to measure the temperature and the heat flux,
- infrared camera and video camera at the upper lid to observe the melt surface,
- vacuum pump to suck the melt out of the vessel to investigate the crust

The features allow to investigate effects, that could not be investigated in the other test facilities, which have been described in the previous chapters. Especially the combination of 3D-geometry, volumetric heating and the possibility to realize several pouring modes, is unique.

5.2 Simulant materials for LIVE experiments

Simulant materials should represent the real core materials in important physical properties and in thermo-dynamic and thermo-hydraulic behavior as accurate as possible. Therefore, the applicability of several binary melt compositions as a simulant melt for the oxidic part of the corium has been checked.

Important criteria for the selection are that the simulant melt should be a non-eutectic mixture of several components with a distinctive solidus-liquidus area of about 100 K, and that the simulant melt should have a similar solidification and crust formation behaviour as the oxidic corium. Moreover, the simulant melt should not be toxic and aggressive against steel and vessel instrumentation. And finally, the temperature range of the simulant melt should not exceed 1000 °C, because of the technical handling and the selection of the volumetric heating system and the heating furnace.

For the first series of experiments a binary mixture of sodium nitrate NaNO_3 and potassium nitrate KNO_3 was chosen (Fig. 5-8). The eutectic composition of this melt is 50-50 Mol% and the eutectic temperature is 225 °C. The maximum temperature range between solidus and liquidus is ~60 K for a 20-80 Mol% NaNO_3 - KNO_3 mixture. This melt can be used in a temperature range from 220 to 380 °C. Due to its solubility for water the applicability of this melt is restricted to dry conditions inside the test vessel.

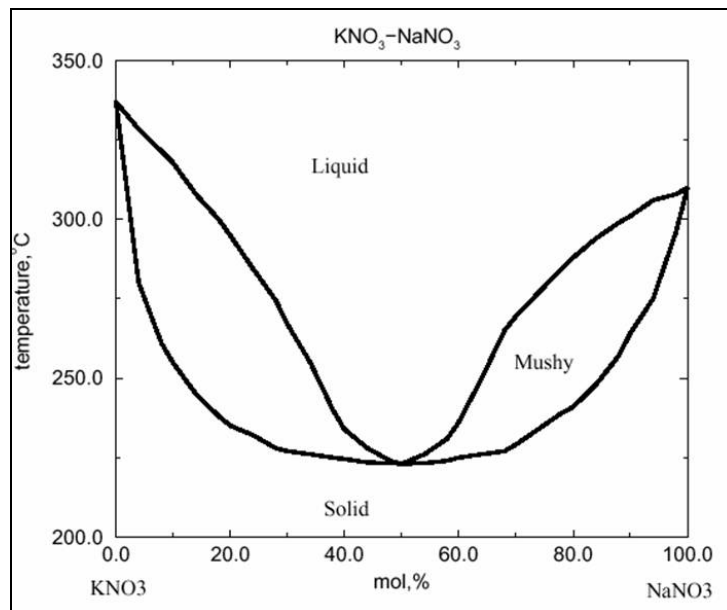


Fig. 5-8: Phase diagram of the KNO_3 - NaNO_3 melt.

For experiments, in which phenomena in the lower head are investigated under presence of water, another simulant melt has to be selected. Therefore several binary oxide melts, which are insoluble in water, have been investigated with respect to their applicability for simulant tests. In the temperature range between 800 and 1000 °C only a few oxides can be considered. These are the oxides MoO_3 and TeO_2 with melting temperatures between 700 and 800 °C and the oxide V_2O_5 with a melting temperature of about 660 °C. The investigations showed that MoO_3 starts to sublime already at about 700 °C and is really aggressive against all types of steel. Both MoO_3 and TeO_2 show a pronounced increase of their vapor

pressure with increasing temperature and are therefore not applicable. As V_2O_5 did not show this behavior, this oxide was chosen as one of the melt constituents. Three binary mixtures with V_2O_5 have been found and were successfully tested with respect to their compatibility with steel: V_2O_5 with CuO , V_2O_5 with ZnO , and V_2O_5 with MgO . In (Fig. 5-9) the phase diagram of the mixture V_2O_5 - ZnO is shown. The eutectic temperature of this mixture is $625^\circ C$.

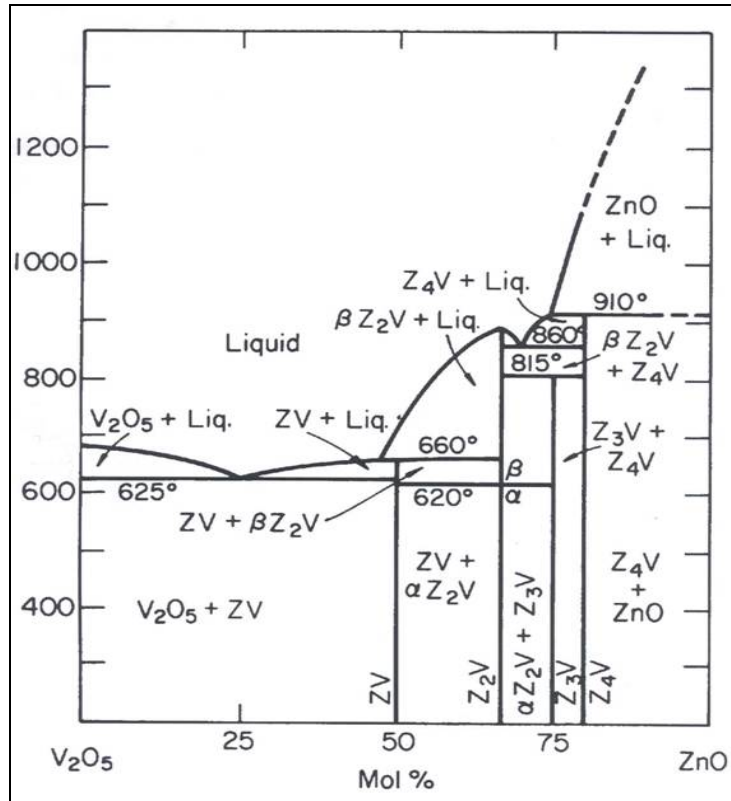


Fig. 5-9: Phase diagram of the V_2O_5 - ZnO melt

Table 5-1 shows the material properties of $NaNO_3$ - KNO_3 mixtures. The values are taken from [Seh01] and [Tou77]. Unfortunately, the data base of the V_2O_5 - ZnO properties is still insufficient.

Table 5-1: Material properties of NaNO₃-KNO₃ mixtures

	NaNO ₃ -KNO ₃ 20:80 Mol%			NaNO ₃ -KNO ₃ 50:50 Mol%			
	Temperature in °C			Temperature in °C			
	300	350	400	250	300	350	400
c _p [J/kgK]	1369 ¹	1369 ¹	1369 ¹	1311	1320 ²	1320 ²	1320
ρ [kg/m ³]	1897,78	1862,76	1827,74	1936,92	1903,12	1869,31	1835,51
η [Pas]	3,32E-03	2,51E-03	1,96E-03	4,64E-03	3,19E-03	2,31E-03	1,80E-03
ν [m ² /s]	1,75E-06	1,35E-06	1,07E-06	2,39E-06	1,68E-06	1,24E-06	9,82E-07
λ [W/mK]	0,439	0,422	0,422	0,474	0,459	0,443	0,422
β [1/K]	3,81E-04 ³	3,81E-04 ³	3,81E-04 ³	3,81E-04 ³	3,81E-04 ³	3,81E-04 ³	3,81E-04 ³
a [m ² /s]	1,69E-07	1,65E-07	1,69E-07	1,87E-07	1,83E-07	1,80E-07	1,74E-07
Pr	10,36	8,14	6,35	12,82	9,18	6,89	5,64

¹from [Seh01] at 316 °C²from [Seh01] at 267 °C³from [Tou77] for NaNO₃ at 550 K

5.3 Phenomena to be investigated in the LIVE test facility

The previous chapters have shown that the most experiments in different test facilities have been performed in 2D slices of different geometry and different aspect ratios (BALI, SIMECO, COPO, RASPLAV), or the internal heat sources were missing (ACOPO). Furthermore the experiments conducted in these facilities were steady-state or quasi steady-state (except the mixing experiments in SIMECO). Moreover, most of the earlier tests have been conducted with hemispheres which were completely filled, and with isothermal outer boundaries. An additional limitation was the lack of information about the melt and vessel behaviour during the melt relocation phase.

To provide the estimate of the remaining uncertainty band under the aspect of safety assessment, the LIVE program has been initiated at FZK. Its main objective is to study the core melt phenomena both experimentally in large-scale 3D geometry and in supporting separate-effects tests. Within the LIVE experimental program large-scale tests in 3D geometry are performed with water and with non-eutectic melts ($\text{KNO}_3\text{-NaNO}_3$) as simulant fluids. The results of these experiments, performed in nearly adiabatic and in isothermal conditions, will allow a direct comparison with findings obtained earlier in other experimental programs (SIMECO, ACOPO, BALI, etc.) and can be used for the assessment of the correlations derived for the molten pool behavior.

With the construction of the LIVE facility several new features were realized, which were not available in the previous experimental facilities, e.g.:

- The melt can be poured into the vessel at different positions with different mass flow rates and at different temperatures. This provides additional information on vessel thermal loadings during the melt pour and its consequences on the long-term behaviour of the crust and the melt incl. heat flux distribution for possible non-symmetric situations. The ability to investigate gradual melt relocation is another advantage.
- The melt pool can be volumetrically heated in a 3D geometry.
- In addition to the “usual” measurements like melt pool temperature and heat flux distribution along the vessel wall, LIVE can provide detailed information about the crust surface and pool/boundary layer interface temperatures dependent on the imposed heat fluxes.
- Extensive post-test analysis includes measurements of the crust thickness profiles along the vessel head, crust composition and morphology. Such data like crust thermal conductivity, crust porosity, distribution of refractory part along the crust thickness have not been studied in detail before. These results (especially in combination with the ongoing ISTC projects with real corium) deliver important information for understanding the solidification of binary non-eutectic melts with reference to reactor situations.

These features allow to carry out new experiments to complement the results obtained earlier in other facilities. Since currently the LIVE1 phase of the program is ongoing (behavior of the molten pool without residual water in the lower head), the phenomena discussed below are related to the tests with molten salt ($\text{NaNO}_3\text{-KNO}_3$) binary melts. They can be divided into

two parts:

1. Phenomena in steady state situations behavior:
 - 1.1. Influence of the pool height on heat fluxes to the vessel wall and the top of the pool
 - 1.2. Comparison of heat fluxes in LIVE with heat fluxes determined in a 2D geometry
 - 1.3. Comparison of heat fluxes in LIVE with heat fluxes determined in ACOPO experiments
 - 1.4. Crust:
 - 1.4.1. Influence of the power density on the crust formation
 - 1.4.2. Influence of pool height on the crust thickness distribution
 - 1.4.3. Influence of the temperature of the cooling water on the crust formation
 - 1.4.4. Influence of the composition of the melt on the crust
 - 1.4.5. Influence of the crust thickness on the Nusselt numbers
2. Phenomena in transient situations:

Transient situations especially affect the crust structure. Several effects should be investigated:

 - 2.1. Influence of the temperature history of the pool on the crust
 - 2.2. Influence of the temperature of the poured melt on the crust
 - 2.3. Influence of the poured mass on the crust
 - 2.4. Influence of the position of the poured melt on the crust
 - 2.5. Behavior of the crust after pouring of additional melt in a pool, which was already in equilibrium

It is possible that during the experimental program new phenomena will be identified, which also have to be investigated. Suggestions about the possible tests in LIVE to address the phenomena described above are given in the following chapter.

Especially the knowledge base for transient situations is still poor. Recently conducted experiments showed for example, that there is a dependence of the crust thickness and composition on the temperature history of the pool. This was not reported in earlier experiments. Because the crust has influence on the heat removal of the pool, this phenomenon has to be investigated in detail.

5.4 Planned experiments in the LIVE test facility

5.4.1 Experiments with water at different pool heights and power densities

These experiments will be done to study the influence of the pool height on heat fluxes to the vessel wall and the top of the pool (phenomenon 1.1 in chapter 5.3).

An experimental series with water as melt simulant can help to clarify, if the correlations for the Nusselt numbers determined in experiments with totally filled hemispheres are also valid, when the hemisphere is only partly filled. This question is important, because a changed split of the heat fluxes changes also the formation of the crust at the wall.

One can expect that in the case of a lower melt height a higher portion of the internally produced heat goes into the upper direction, because the ratio of the area of the top of the pool to the area of the interface between pool and wall increases in this case (see Fig. 1-1, h^* is the normalized height of the pool, e.g. $h^*=h/R$). Otherwise, the Rayleigh number decreases, which changes the flow regime.

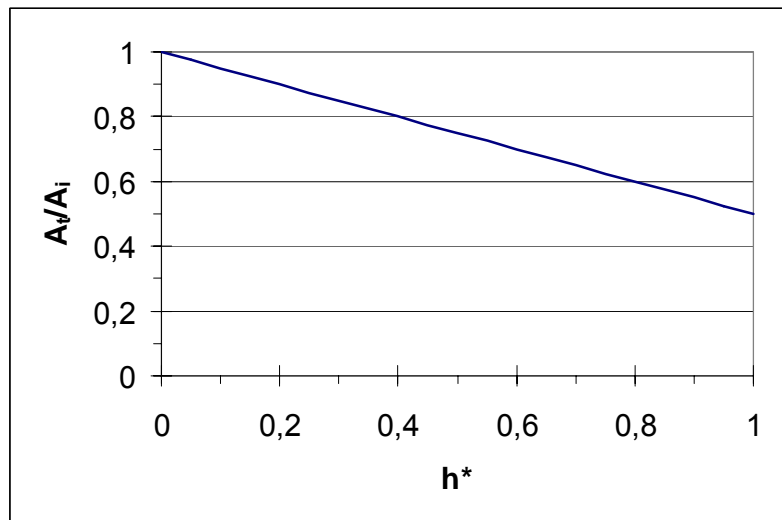


Fig. 1-1: Ratio of the area at the top of the pool to the area at the interface with the wall vs. the normalized height of the pool

The experiments are relatively easy to realize. The main parameters that have to be determined are the fluid temperature distribution and the heat flux through the vessel wall at different pool heights and power levels.

5.4.2 Experiments with water in the LIVE vessel and in a slice with the same radius

Comparison of 3D heat fluxes in LIVE with heat fluxes determined in 2D geometry (phenomenon 1.2 in chapter 5.3).

As it has been described in previous sections, most of the correlations for the steady state upwards and downwards heat transfer in the pool were determined in experiments with slice geometry. However the validity of these correlations for hemisphere geometry has to be demonstrated. Therefore, results from water experiments in the LIVE vessel will be compared with results from experiments in slices at similar boundary conditions.

5.4.3 Cooling down hot water in the LIVE vessel like in ACOPO experiments

In this experiment, the phenomenon 1.3 in chapter 5.3 should be investigated.

This experiment serves the comparison of heat fluxes in LIVE with heat fluxes determined in ACOPO.

The ACOPO experiments are described in chapter 3.4. The water in the vessel was cooled down and a Rayleigh number was derived from the heat flux through the vessel wall and the temperature distribution in the melt.

Comparing these results with results obtained from experiments with different water level in the vessel and different volumetric heat release, the philosophy which underlies the ACOPO experiments can be addressed.

5.4.4 Experiments with $\text{NaNO}_3\text{-KNO}_3$ to confirm the results in the SIMECO facility

Investigated phenomena (see chapter 5.3): 1.2., 1.4.1., 1.4.5.

Experiments with the salt mixture $\text{NaNO}_3\text{-KNO}_3$ have been performed earlier in the SIMECO facility at KTH (Sweden) [Kol00]. In Table 1-1 the experimental results of the SIMECO tests are summarized

Table 1-1: Experimental results in SIMECO tests with $\text{NaNO}_3\text{-KNO}_3$ salts

Material	Experiment	Ra'	Nu_{up}	Nu_{down}	Nu_{up}/Nu_{down}
$\text{NaNO}_3\text{-KNO}_3$ (50%-50%)	SSEu-12	8,610E+12	298,7	153,4	1,947
	SSEu-13	4,160E+12	316,3	150,6	2,100
$\text{NaNO}_3\text{-KNO}_3$ (20%-80%)	SNEu-01	1,389E+13	246,4	143,0	1,723
	SNEu-03	3,620E+12	167,4	101,6	1,648
	SNEu-04	6,760E+12	149,7	128,6	1,164
	SNEu-06	6,040E+12	173,7	152,5	1,139
	SNEu-07	1,196E+13	295,0	175,6	1,680

These results are given in Fig. 1-2.

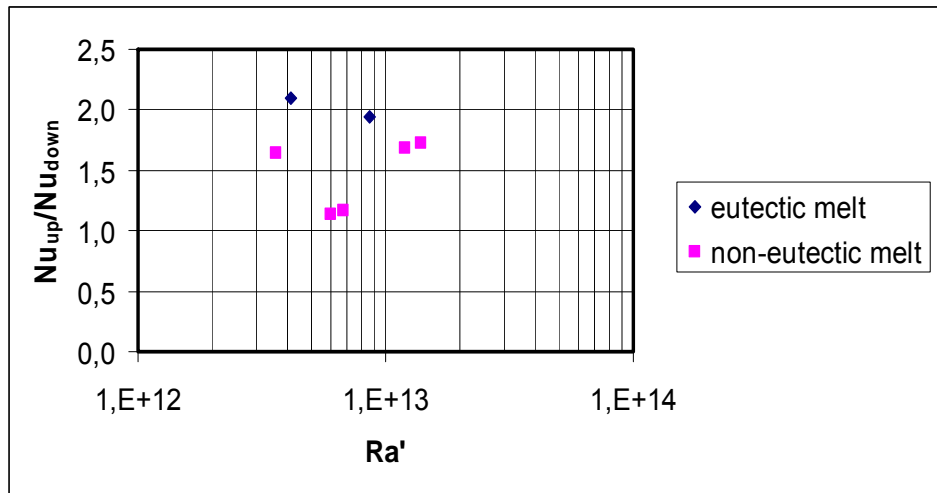


Fig. 1-2: Experimental results in SIMECO tests with NaNO₃-KNO₃ salts

It is possible to determine the Rayleigh number from the power and the melt temperature. This is shown in Fig. 1-3 and Fig. 1-4 for both salt mixtures (20%-80% and 50%-50%) used in the LIVE facility. A height of the melt of 43 cm is assumed.

In the experiments, which can be conducted with the eutectic and the non-eutectic mixtures, the solid mixture of the respective salt at room temperature can be heated up increasing the power successively. When the steady state is reached at a certain power level, the material parameters can be determined from the measured temperature. Using these values of the material parameters the “effective” Ra numbers can be determined.

Other parameters to be determined are:

- The heat flux to the upper side of the pool and into the vessel wall
- Thickness of the crust, if possible, dependent on the angle in the lower head

Using these results it is possible to compare the Nusselt numbers at the upper side with the Nusselt numbers at the vessel wall. It is also possible to compare the relation of these Nusselt numbers with the results in the SIMECO tests (see Fig. 1-2). The crust thickness can also be compared.

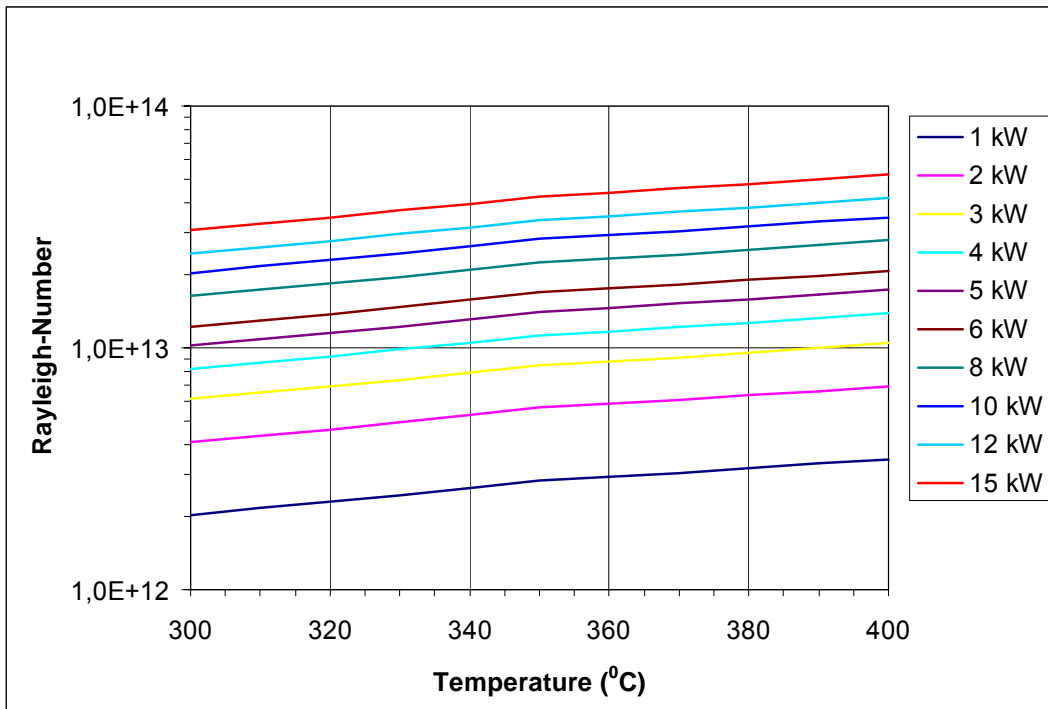


Fig. 1-3: Rayleigh numbers vs. Temperature for the non-eutectic (20%-80%) $NaNO_3-KNO_3$ mixture

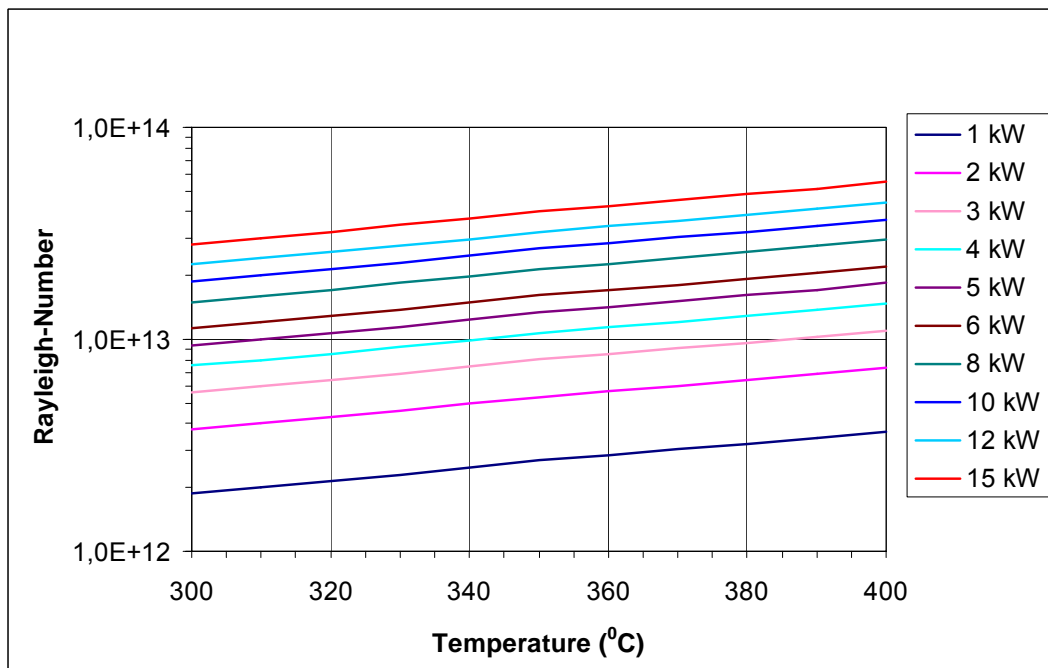


Fig. 1-4: Rayleigh numbers vs. Temperature for the eutectic (50%-50%) $NaNO_3-KNO_3$ mixture

5.4.5 Experiments with $\text{NaNO}_3\text{-KNO}_3$ at different power densities

Investigated phenomenon ([see chapter 5.3](#)): 1.4.1.

The main objective in these tests is to determine the influence of heat generation on crust growth. Several power levels have to be applied and the crust thickness has to be measured after reaching the steady state conditions. If possible the correlation between the crust thickness and the heat flux through the wall has to be derived.

5.4.6 Experiments with $\text{NaNO}_3\text{-KNO}_3$ at different heights of the melt

Investigated phenomena ([see chapter 5.3](#)): 1.1., 1.4.2.

Study of the melt behavior for different melt pool height has to be performed with $\text{NaNO}_3\text{-KNO}_3$ non-eutectic and eutectic mixtures. Besides the upwards and downwards heat fluxes the formation of the crust can be investigated in these experiments.

5.4.7 Experiments with $\text{NaNO}_3\text{-KNO}_3$ at different cooling conditions

Investigated phenomenon ([see chapter 5.3](#)): 1.4.3.

The crust formation and behavior has to be investigated for different cooling conditions at the outer vessel wall. At least two tests with two different conditions at the outside vessel wall are necessary. In the first one the mass flow rate of the cooling water and power density has to be varied. However, this will provide different temperature conditions at the outer surface (from almost isothermal at high mass flow rate to a temperature distribution at low mass flow rate). In the second test boiling conditions at the outer side of the vessel wall have to be established.

5.4.8 Experiments with $\text{NaNO}_3\text{-KNO}_3$ at different compositions of the melt

Investigated phenomenon ([see chapter 5.3](#)): 1.4.4.

The main objective of these experiments is to compare the crust formation and behavior for non-eutectic and eutectic binary melts. Naturally, all other initial and boundary conditions (cooling, power density, height of melt pool) have to be the same in both tests.

5.4.9 Experiments with $\text{NaNO}_3\text{-KNO}_3$ in the LIVE vessel and in a slice with the same radius

Investigated phenomena (see chapter 5.3): 1.2., 1.4.

To demonstrate the influence of geometric effects, selected LIVE 3D experiments have to be repeated in the slice geometry. All important parameters of the slice test section (e.g. volumetric heat generation, cooling conditions and instrumentation) have to be as close to the LIVE 3D vessel as possible.

5.4.10 Experiments with $\text{NaNO}_3\text{-KNO}_3$ with different time histories

Investigated phenomenon (see chapter 5.3): 2.1.

The final steady state conditions at a unique temperature of the $\text{NaNO}_3\text{-KNO}_3$ mixture have to be reached over different ways. It is, for example, possible to heat the melt with a lower power density from the beginning in one experiment. In a second experiment, one heats the melt at the beginning with a high power density and reduces the power density later to the same level as in the first experiment. The crusts of these two experiments have to be compared.

5.4.11 Experiments with $\text{NaNO}_3\text{-KNO}_3$ with different initial pouring temperatures of the melt

Investigated phenomenon (see chapter 5.3): 2.2.

The main objective of these tests is to study the initial conditions of the melt relocation to the lower plenum. The parameter to be varied is the temperature of the melt (e.g. well above the liquidus or between the liquidus and solidus to promote rapid crust formation at the vessel wall). The constant parameters are: poured mass, position of pouring, heating power in the vessel, wall temperature of the vessel. Besides the heat fluxes the crust formation at the vessel wall and at the top of the pool has to be investigated.

5.4.12 Experiments with $\text{NaNO}_3\text{-KNO}_3$ with different pouring masses

Investigated phenomenon (see chapter 5.3): 2.3.

The preheated $\text{NaNO}_3\text{-KNO}_3$ mixture has to be poured into the vessel. The mass of the poured melt has to be varied in different tests of the series. The constant parameters are: position of pouring, heating power density in the vessel, wall temperature of the vessel, temperature of the poured mass. Besides the heat fluxes the crust formation at the vessel wall and the top of the pool has to be investigated.

5.4.13 Experiments with $\text{NaNO}_3\text{-KNO}_3$ with different melt pouring positions

Investigated phenomenon ([see chapter 5.3](#)): 2.4.

The preheated $\text{NaNO}_3\text{-KNO}_3$ mixture has to be poured into the vessel. The position of pouring has to be varied in different tests of the series. The constant parameters are: poured mass, heating power in the vessel, wall temperature of the vessel, temperature of the poured mass. Besides the heat fluxes the crust formation at the vessel wall and the top of the pool has to be investigated.

5.4.14 Experiments with $\text{NaNO}_3\text{-KNO}_3$ with a gradual pouring of melt

Investigated phenomenon ([see chapter 5.3](#)): 2.5.

The preheated $\text{NaNO}_3\text{-KNO}_3$ mixture has to be poured into the vessel gradually. By comparison with other experiments the influence of the pouring process on the crust formation can be investigated. The constant parameters are: position of pouring, total mass of poured melt, temperature of poured melt, heating power density in the vessel, wall temperature of the vessel.

6 REFERENCES

- [And89] James L. Anderson, James J. Sienicki, Thermal behavior of molten corium during the Three Mile Island Unit 2 core relocation event, Nuclear Technology, Vol. 87 (1989), 283-293
- [Asm98a] V. Asmolov et al., Experimental study of heat transfer in the slotted channels at CTF facility, OECD/CSNI Workshop on In-Vessel Core Debris Retention and Coolability, Garching, Germany, March 3-6, 1998
- [Asm98b] V. Asmolov et al., Results of salt experiments performed during phase I of RAS-PLAV project, published in January, 1998
- [Asm00] V. Asmolov et al., RASPLAV Final Report, published in 2000
- [Asm01] V. Asmolov et al., Challenges left in the area of in-vessel melt retention, Nucl. Eng. Des. 209 (2001), pp. 87-96
- [Band98] G. Bandini et al., Molten material relocation into the lower plenum: a status report September 1998, report no. NEA/CSNI/R(97)34
- [Band01] G. Bandini, Synthesis paper on the status of degraded core issues, report no. NEA/CSNI/R(2001)5, 2001
- [Ber98] L. Bernaz et al., Thermalhydraulic Phenomena in Corium Pools: Numerical Simulation with TOLBIAC and Experimental Validation with BALI, OECD/CSNI Workshop on In-Vessel Core Debris Retention and Coolability, Garching, Germany, March 3-6, 1998
- [Chu75] S. W. Churchill, H. S. Chu, Correlating equations for laminar and turbulent free convection from a vertical plate, Int. J. Heat Mass Transfer, Vol. 18 (1975), 1323-1329
- [Chu99] Y.T. Chu et al., Lower Head Failure Experiments and Analyses, NUREG/CR-5582/Feb., 1999
- [Fzk08] Homepage of LIVE Test Facility on FZK server:
<http://www.iket.fzk.de/cube/index.php?pid=fc8bb2598808cf311c54c84a475aaaf1>
- [Glo59] S. Globe, D. Dropkin, Natural- Convection Heat Transfer in Liquids Confined by Two Horizontal Plates and Heated From Below, J. Heat Transfer 81 (1959), 24-28
- [Hel99] M. Helle et al., Experimental COPO II data on natural convection in homogenous and stratified pools, 9th Inter. Topical Meeting on Nuclear Reactor Thermal-Hydraulics (NURETH-9), San Francisco, October 3-8, 1999
- [Hof94] P. Hofmann et al., Essential experimental result of the CORA test program on severe code damage phenomena, Kerntechnik 59 (1994), p. 197
- [Huh99] I. Huhtiniemi, D. Megallon, Insight to steam explosion with corium melts in KROTOS, 1999

REFERENCES

- [Kim98] H. D. Kim, S.B. Kim, Overview of severe accident research and SONATA-IV phase-I experiment at KAERI, presented at CSARP, Bethesda, Maryland, May 4-7, 1998
- [Kol00] G. Kolb, S. A. Theerthan, B.R. Sehgal, Experiments on In-Vessel Melt Pool Formation and Convection with $\text{NaNO}_3\text{-KNO}_3$ salt mixtures as melt simulates, 8th Intern. Conf. on Nucl. Engin. (ICONE 8), Baltimore, MD, April 2-6, 2000
- [Kym97] O. Kymäläinen, H. Tuomisto and T.G. Theofanous, In-Vessel retention of corium at the Loviisa-plant, Nucl. Eng. Des. 169 (1997), 109-130
- [Kym03] Kymäläinen et al., Heat flux distribution from a volumetrically heated pool with high Rayleigh number, 6th Inter. Topical Meeting on Nuclear Reactor Thermal-Hydraulics (NURETH-6), Seoul, Korea, October 5-8, 2003
- [May75] F. Mayinger et al., Untersuchung thermohydraulischer Vorgänge sowie Wärmeaustausch in der Kernschmelze, Bundesministerium für Forschung und Technologie, Abschlußbericht RS48/1, 1975
- [Meg99] D. Megallon, I. Hutiniemi, Corium melting tests at low pressure and subcooled water in FARO, 9th Inter. Topical Meeting on Nuclear Reactor Thermal-Hydraulics (NURETH-9), October 3-8, 1999
- [Mia07] A. Miassoedov, Thomas Cron, Jerzy Foit, Results of the LIVE-L2 experiment on melt behaviour in RPV Lower Head performed within the LACOMERA Project at the Forschungszentrum Karlsruhe, 15th Intern. Conf. On Structural Mechanics in Reactor Technology (Smirt-19), Toronto, Canada, August 12-17, 2007
- [Sar07] 2nd DRAFT of Contract EC-SARNET/FI6O-CT-2004-509965, Evaluation of Severe Accident Research Priorities, May 2007
- [Sch99] G. Schwarz et al., Applicability of PHEBUS FP results to Severe Accident Safety Evaluation and Management Measures. FSA-99, Luxembourg, November 29 – December 1, 1999
- [Seh99] B. R. Sehgal et al., FOREVER experimental program in pressure vessel creep behavior and core debris retention. 15th Intern. Conf. On Structural Mechanics in Reactor Technology (SmiRT-15), Seoul, Korea, August 15-20, 1999
- [Seh01] B.R. Sehgal, Z.L. Yang, Ex-vessel core melt stabilization research – On the experiments with simulant materials at KTH, report to contract FIKS-CT1999-00003 in the frame of the ECOSTAR project, January 2001
- [Seh03] B.R. Sehgal et al., Assessment of Reactor Vessel Integrity (ARVI), Nucl. Eng. Des. 221 (2003), 23-53
- [Seh04a] B.R. Sehgal, H.S. Park, Pre-Project on development and validation of melt behaviour in severe accidents, report NKS-99, ISBN 87-7893-158-4, 2004
- [Seh04b] B.R. Sehgal et al. Phenomenological studies on melt –structure-water interaction (MSWI) during postulated severe accidents : year 2004 activity, SKI Report 2005:42

-
- [Ste78] U. Steinberner, H. H. Reineke, Turbulent buoyancy convection heat transfer with internal heat sources, Proc. 6th International Heat Transfer Conf., Toronto, Canada, August 7-11, 1978
- [Ste05] A. V. Stepanyan, A. K. Nayak, B. R. Sehgal, Experimental investigations of natural convection in three layer stratified pool with internal heat generation, 11th Inter. Topical Meeting on Nuclear Reactor Thermal-Hydraulics (NURETH-11), Avignon, France, October 2-6, 2005
- [The97] T.G. Theofanous et al., The first results from the ACOPO experiments, Nucl. Eng. Des. 169 (1997), 49-57
- [The00] S. A. Theerthan et al., The role of phase separation on heat transfer in internally heated liquid layers, Proc. of 8th Intern. Conf. on Nucl. Eng. (ICONE 8), Baltimore, MD April 2-6, 2000
- [The01] T.G. Theofanous, S. Angelini, Natural convection for in-vessel retention at prototypic Rayleigh numbers, Nucl. Eng. Des. 200 (2001), pp. 1-9
- [Tou77] Y.S. Touloukian et al., Thermophysical properties of matter, The TPRC data series, volume 13, New York, 1977
- [Yan99] Z.L. Yang et al., Experimental investigation on dryout heat flux of a particle debris bed with a downcomer. OECD Workshop on Ex-vessel Debris Coolability, Karlsruhe, Germany, 16.11.-18.11.1999

Appendix A

Experimental facilities

	COPO I	COPO II	BALI	SIMECO	ACOPO	RASPLAY-salt	LIVE
Institution	Fortum Nuclear Services (Finland) and CEA/DRN (Grenoble)	CEA (Grenoble)	CEA (Grenoble)	KTH (Stockholm)	Univ. of California, Santa Barbara	Kurchatov Institute (Russia)	FZK (Karlsruhe)
Investigated Effects	- Heat transfer in a melt pool undergoing natural convection - Heat transfer phenomena in a stratified melt pool undergoing natural convection - Crust effects on heat transfer	- Heat transfer in a melt pool undergoing natural convection - Heat transfer phenomena in a stratified melt pool undergoing natural convection - Crust effects on heat transfer	- Heat transfer phenomena in a stratified melt pool undergoing natural convection - Focussing effect of a metallic layer at the top of oxidic pool	- Heat transfer phenomena in a stratified melt pool undergoing natural convection - Crust formation	- Heat transfer in a melt pool undergoing natural convection	- Heat transfer in a melt pool undergoing natural convection - Crust formation	- Heat transfer in a melt pool undergoing natural convection - Crust formation - Influence of conditions during melt relocation (temperature, position, mass etc.) on crust formation - 3D-effects
Geometry	- Curved slice - Radius: 0,885 m - Thickness: 10 cm	- Curved slice - Radius: 1 m - Thickness: 9,4 cm	- Curved slice - Radius: 2 m - Thickness: 15 cm	- Curved slice - Radius: 25 cm - Thickness: 9 cm	- Hemisphere - Radius: 1 m	- Curved slice - Radius: 20 cm - Thickness: 16,7cm	- Hemisphere - Radius: 0,5 m
Scale	1:2 (Loviisa)	1:2 (Loviisa, AP 600)	1:1 (Prototyp. French PWR)	1:8 (AP 600)	1:2 (AP 600)	1:10	1:5 (Prototyp. German PWR)
Heating	Direct joule heating	Direct joule heating	Direct joule heating	coil type heater, submerged in the liquid	no heating	Side wall heating, Direct joule heating	Volumetrical heating by shrouded electrical resistance wires
Material	Melt: $H_2O-ZnSO_4$ -Solution Coolant: Water	Melt: $H_2O-ZnSO_4$ -Solution (corium) Distilled water (metal layer) Coolant: Liquid nitrogen	Melt: Salted water Coolant: Organic liquid	Melt: Chlorobenzene (for U-Fe) -Water (for U), -Paraffin (for Zr), - $NaNO_3-KNO_3$ Coolant: Water	Melt: Water Coolant: Water	Melt: NaF-NaBF ₄ mixtures Coolant: $NaNO_2-NaNO_3-KNO_3$	Melt: Water, $NaNO_3-KNO_3$, V_2O_5 Coolant: Water
Temperature	10-80°C	10-80°C	10-80°C	10-80°C (Water)	10-80°C	400-600°C	200-250°C ($NaNO_3-KNO_3$) 1000-1500°C (V_2O_5)
Ra-Range	$10^{12} - 10^{13}$	$10^{12} - 10^{13}$	$10^{16} - 10^{17}$	$6 \cdot 10^{12} - 2 \cdot 10^{13}$	Up to 10^{17}	$2 \cdot 10^{11} - 2 \cdot 10^{13}$	$10^{10} - 10^{11}$
Flow Regime	turbulent	turbulent	turbulent	turbulent	turbulent	turbulent	turbulent
Time Regime	steady state	steady state	steady state	steady state	steady state	steady state	steady state/ transient

Appendix B

EURSAFE Research Issue and Rationale for Selection (from [Sar07])

Issue for needed Re-search	Rationale for selection	Revised Priority	Expected benefit
FCI incl. steam explosion in weakened vessel	Investigate the risk of weakened vessel failure during re-flooding of a molten pool in the lower head.	CL	
Containment atmosphere mixing and hydrogen combustion / detonation	Identify the risk of early containment failure due to hydrogen accumulation leading to deflagration / detonation and to identify counter-measures.	H	Optimisation of the implementation of hydrogen mitigation measures such as PAR
Dynamic and static behaviour of containment, crack formation and leakage at penetrations	Estimate the leakage of fission products to the environment.	open	
Direct containment heating	Increase the knowledge of parameters affecting the pressure build-up due to DCH and determine the risk of containment failure.	M	
Oxidising environment impact on source term	Quantify the source term, in particular for Ru, under oxidation conditions / air ingress for HBU and MOX.	H	Include air ingress in source term and PSA
Aerosol behaviour impact on source term	Quantify the source term for aerosol retention in the secondary side of steam generator and leakage through cracks in the containment wall as well as the source into the containment due to re-volatilization in RCS.	L	
RCS high temperature chemistry impact on source term	Improve predictability of iodine/Ru species exiting RCS to provide the best estimate of the source into the containment.	H	Possible reduction of conservatism in source term assessment used for emergency preparedness
Containment chemistry impact on source term	Improve the predictability of iodine chemistry in the containment to reduce the uncertainty in iodine source term.	H	Possible reduction of conservatism in source term assessment used for emergency preparedness

Issue for needed Re-search	Rationale for selection	Revised Priority	Expected benefit
Core re-flooding impact on source term I	Characterise and quantify the FP release during core re-flooding.	L	

Column 'Revised Priority':

- H - high research priority
- M - medium priority, programs to be continued as planned or at reduced effort
- L - low priority/second priority, no further new activities in SARNET frame, but continued in other research programs outside SARNET
- CL - 'issue could be closed'. From point of risk significance and state of knowledge no further experimental program needed